



Cite this: *RSC Adv.*, 2025, **15**, 14691

Received 15th January 2025
 Accepted 29th March 2025

DOI: 10.1039/d5ra00361j
rsc.li/rsc-advances

Advances and developments in transition metal-free benzylic $C(sp^3)$ –H activation/functionalization reactions

Fatemeh Doraghi, ^a Shahab Kermaninia, ^b Elika Salehi Ghalehsefid, ^b Bagher Larijani^a and Mohammad Mahdavi ^{*a}

Transition metal-free $C(sp^3)$ –H activation of toluene derivatives is known as a green and sustainable methodology for constructing carbon–carbon and carbon–heteroatom bonds. Benzylic $C(sp^3)$ –H activation/functionalization bond formation can be carried out in the presence of organic/inorganic peroxides, bases, acids, and other radical initiators. These radical transformations also occur under photochemical and electrochemical conditions. In this review, we highlight the C–H activation/annulation or C–H activation/functionalization reactions of benzylic carbon atoms in the presence of non-metal catalysts or promoters or without any catalyst.

1. Introduction

Direct formation of carbon–carbon or carbon–heteroatom bonds without the use of transition metals has been a topic of interest for synthetic chemists for years.^{1–4} The use of transition metal catalysts in oxidative reactions is limited owing to their high cost, sensitivity to oxygen and humidity, and also potential toxicity. Researchers have investigated metal-free radical reactions, where radical species are typically produced using an oxidant under mild reaction conditions. These reactions show

high reaction activity and excellent tolerance towards various functional groups.^{5,6} In direct oxidative transformations, terminal oxidants play an important role in promoting the reaction.⁷ Over the years, various organic and inorganic oxidants have been employed in oxidative processes.

As the benzylic groups are synthetically relevant fragments, the direct activation and functionalization of these $C(sp^3)$ –H bonds will expand a variety of value-added products for many applications.^{8–10} Although the high bond-dissociation energy (BDE) and low polarity of unactivated $C(sp^3)$ –H bonds make the activation of these bonds challenging in synthetic chemistry, various efforts have been successfully made for the $C(sp^3)$ –H activation of benzylic moieties towards the synthesis of various pharmacologically active compounds.^{11–15} For example, in the

^aEndocrinology and Metabolism Research Center, Endocrinology and Metabolism Clinical Sciences Institute, Tehran University of Medical Sciences, Tehran, Iran.
 E-mail: momahdavi@tums.ac.ir

^bSchool of Chemistry, College of Science, University of Tehran, Tehran, Iran



Fatemeh Doraghi

as a Researcher at the Endocrinology and Metabolism Research Center, Tehran University of Medical Sciences, Tehran, Iran.

Fatemeh Doraghi received her Bachelor and Master degrees in Organic Chemistry from Shahid Chamran University, Ahvaz in 2008 and 2014, respectively. She received her PhD degree in Organic Chemistry from the University of Tehran, Tehran in 2022. During her PhD research, she focused on the development of new synthetic methodologies via transition metal and metal-free oxidative coupling reactions. She is currently employed



Shahab Kermaninia

Shahab Kermaninia was born in 1994 in Karaj, Iran. He received his BSc degree from the Sharif University of Technology in 2017 and his MSc degree from the University of Tehran in 2019. Currently, he is a PhD student with Prof. S. M. Farnia at the University of Tehran. His research interests focus on the transition metal-catalyzed C–H activation and screening approaches.

last decade, there has been a great growth in the transition metal-free oxidative transformations involving toluene derivatives.^{16,17} Some bioactive molecules with benzylic motifs are illustrated in Scheme 1.

In this review, we describe the literature on the activation/functionalization of the benzylic C(sp₃)-H bonds towards the formation of carbon–carbon bonds and carbon–heteroatom bonds and cyclization reactions. The content is classified based on the types of non-metallic catalysts and promoters. The features of the reactions and the challenging mechanisms are also discussed.

2. Benzylic C(sp³)-H activation/functionalization

Organic peroxides exhibit versatile reactivity, enabling reactions to occur at high temperatures, and they act as effective primary oxidants at room temperature under UV or visible light



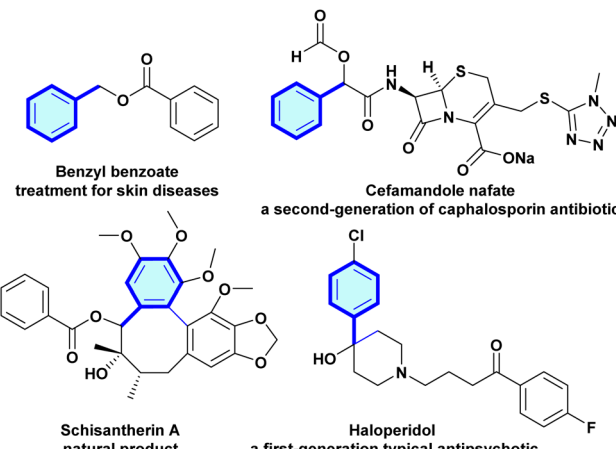
Erika Salehi Ghalehsefid

medicinal compounds at the Endocrinology and Metabolism Research Center, Tehran University of Medical Sciences, Tehran, Iran.



Bagher Larijani

Erika Salehi Ghalehsefid was born in 1999 in Ahwaz, Iran. She received her Master's degree of Science in Organic Chemistry from the University of Tehran, Tehran in 2025. Her thesis was on the design, synthesis, and molecular dynamics of 1,2,4-triazin/chalcone hybrids and investigating the effect of inhibiting alpha-glucosidase enzyme in the treatment of type 2 diabetes. Currently, she is focused on the development of new medicinal compounds at the Endocrinology and Metabolism Research Center, Tehran University of Medical Sciences, Tehran, Iran.



Scheme 1 Some bioactive molecules with a benzylic motif.

irradiation. Both heat and photo-irradiation can easily break the O–O bonds in peroxides owing to the steric repulsion between two oxygen atoms. The resulting active species have a short lifetime and readily oxidize other organic compounds in the reaction medium.^{18,19} Organic peroxides have been used for years as promoters in C(sp₃)-H activation reactions of toluene derivatives.

2.1. C(sp³)-H functionalization using peroxides

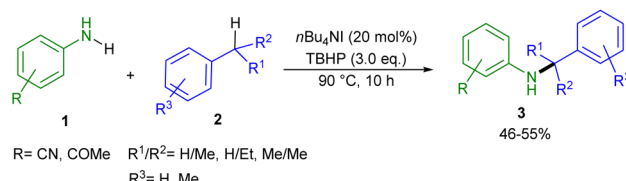
2.1.1. C(sp³)-H functionalization using TBHP. In 2014, Wang and co-workers employed *n*Bu₄NI/TBHP as an efficient oxidative system for direct amination of allylic and benzylic C(sp₃)-H bonds 2 with anilines 1 towards the synthesis of *N*-substituted anilines 3 (Scheme 2).²⁰ It is important to note that no appropriate product was observed in the presence of organic and inorganic oxidants. Using solvents also caused no improvement in this reaction, and the best result was achieved under solvent-free conditions. Considering the mechanism in Scheme 3, *n*Bu₄NI was oxidized by TBHP to generate the iodine



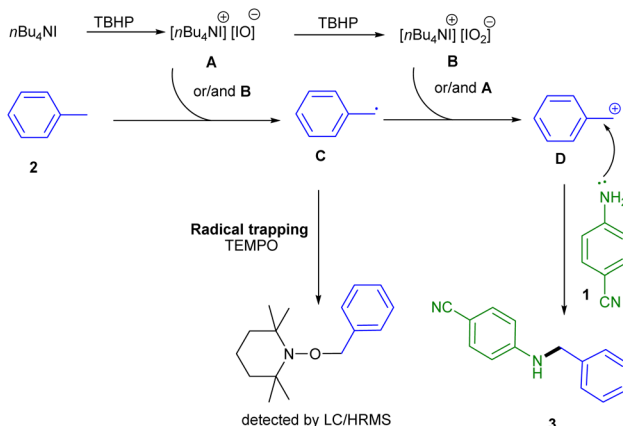
Mohammad Mahdavi

Mohammad Mahdavi was born in 1981 in Tehran, Iran. He received his MSc from the University of Tehran in 2008 and PhD degree in Medicinal Chemistry from the Tehran University of Medical Science, Tehran, Iran, in 2016. Since August 2017, he has been with the Endocrinology and Metabolism Research Center, Endocrinology and Metabolism Clinical Sciences Institute, Tehran University of Medical Sciences, Tehran, Iran where he is an Assistant Professor. His current research interests focus on the synthesis of heterocyclic compounds with biological activities.





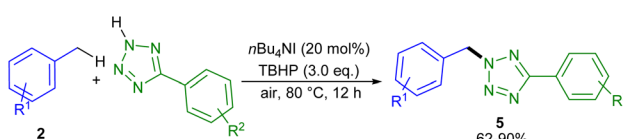
Scheme 2 Direct amination of allylic and benzylic $C(sp^3)$ -H with anilines (Wang and co-workers).²⁰



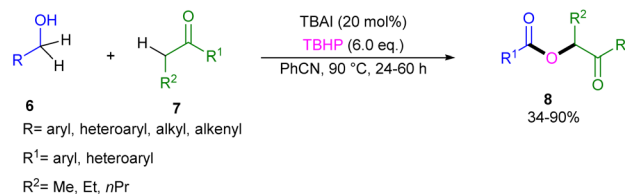
Scheme 3 Possible mechanism for the direct amination of allylic and benzylic $C(sp^3)$ -H with anilines.

species ammonium hypoiodite **A** or iodite **B**. These active intermediates then reacted with toluene **2** to generate the benzyl radical **C**, which by further oxidation furnished the benzyl cation **D**. Then, **D** under the nucleophilic attack of amine **1** provided product **3**. The reason for the high regioselectivity of the reaction could be attributed to the stability of the free radical of benzyl and the steric effect. The amination of allylic and benzylic $C(sp^3)$ -H bonds **2** can be carried out using aryl tetrazoles **4** under an $nBu_4NI/TBHP$ catalytic system (Scheme 4).²¹ The reaction in the presence of BHT (2,6-di-*tert*-butyl-4-methylphenol) as a radical scavenger confirmed the involvement of a radical route, and a deuterium experiment using $[D_8]$ -toluene suggested that $C(sp^3)$ -H cleavage is the rate-determining step. The gram-scale synthesis of product (1.70 g, 72%) demonstrated the synthetic utility of this amination reaction.

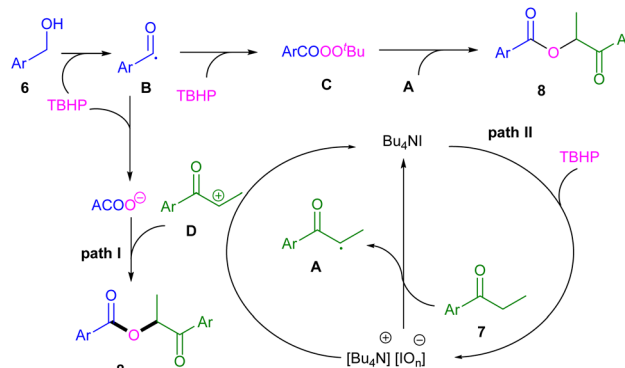
The Cheng group employed TBAI as the catalyst for the reaction of ketones **7** with benzylic alcohols **6** to produce α -acyloxy carbonyl scaffolds **8** in the presence of TBHP as



Scheme 4 $nBu_4NI/TBHP$ -catalyzed amination of benzylic $C(sp^3)$ -H with aryl tetrazoles (Wang and co-workers).²¹

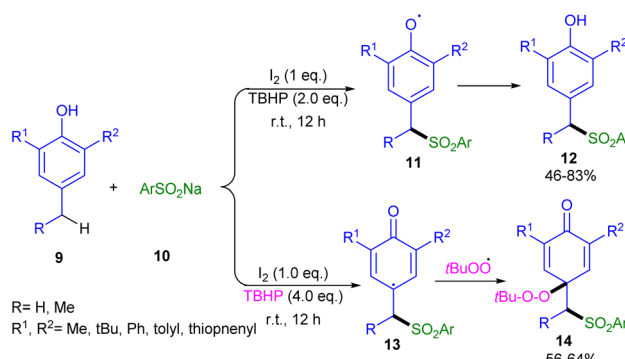


Scheme 5 Coupling of ketones with benzylic alcohols (Cheng and co-workers).²²



Scheme 6 Possible mechanism for the coupling of ketones with benzylic alcohols.

a commercially available oxidant in PhCN as a solvent (Scheme 5).²² The reaction proceeded in moderate yields in EtOAc and MeCN. The radical trapping experiment by using TEMPO proposed the involvement of a radical pathway in this synthetic method. Initially, the oxidation of TBAI by TBHP led to $[Bu_4N]^+[IO_4]^-$, which abstracted a hydrogen atom from ketone to generate the α -carbonyl radical **A**. At the same time, benzylic alcohol was oxidized to benzoyl radical **B** by TBHP. Afterward, **A** reacted with the *tert*-butyl perester **C** to provide the desired product **8**. In another pathway, the oxidation of α -carbonyl radical **A** by $[Bu_4N]^+[IO_4]^-$ forms cation **D**, which reacted with carboxylic anion **C** to deliver product **8** (Scheme 6). It was noteworthy that both radical pathways could be possible.

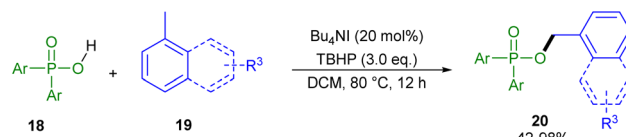


Scheme 7 Metal-free sulfonylation and peroxidative bifunctionalization of phenols (Wu and co-workers).²³



The Wu group reported a mild procedure involving I_2 /TBHP-mediated benzylic $C(sp^3)$ -H sulfonylation of phenol derivatives **9** (Scheme 7).²³ Using 2 equiv. of TBHP and 1 equiv. of I_2 , the desired products were obtained in moderate to high yields with high regioselectivities. In addition, they could achieve a sulfonylative and peroxidative bifunctionalization of phenol derivatives **9** by increasing the amount of TBHP from 2 equiv. to 4 equiv, yielding bifunctionalized ketone products in 56–64% of yield. Screening of other oxidants such as DTBP, DCP, TBPB and H_2O_2 was not effective in this $C(sp^3)$ -S bond formation, and KI, TBAI, I_2O_5 and NIS as iodine additives led to lower product yields. A radical pathway was suggested due to the suppression of the product in the presence of TEMPO as a radical scavenger. Two radical intermediates, the carbon radical **11** and the oxygen radical **13**, were suggested for the construction of products **12** and **14**, respectively. These intermediates can resonate with each other.

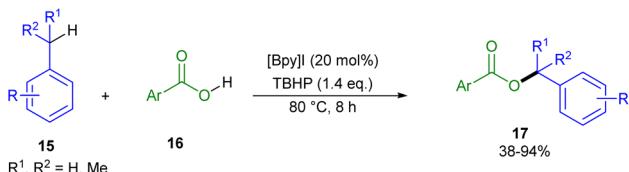
In 2017, the Liu group reported a strategy for the direct oxidative esterification of the $C(sp^3)$ -H bond in benzylic hydrocarbons **15** with carboxylic acids **16** using a heterocyclic ionic liquid as a catalyst (Scheme 8).²⁴ 1-Butylpyridinium iodide catalyst was easily recycled and reused for four cycles without any obvious loss of catalytic activity. According to the tentative mechanism in Scheme 9, **A** or **B** species were generated from the oxidation of $[BPY]I$ by TBHP. Then, the hemolytic cleavage of a benzylic C-H bond in the presence of **A** or **B** produced the benzyl radical **C**, which subsequently combined with benzoic acid to form the radical anion **F**. In path I, product **17** was



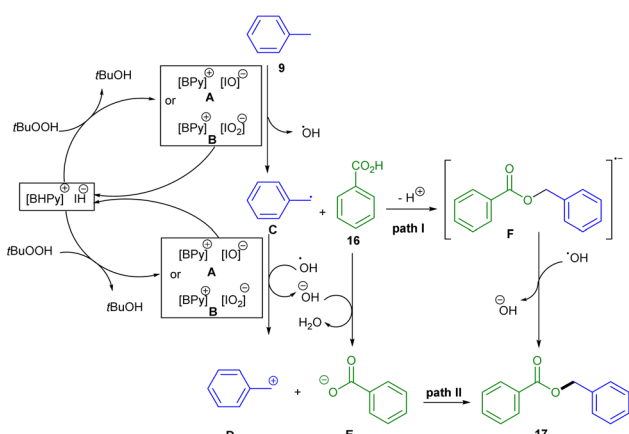
Scheme 10 Coupling of arenes with diaryl phosphinic acids (Xiong and co-workers).²⁵

obtained by losing an electron from **F** with the help of $\cdot OH$. However, **A** or **B** species oxidized the benzyl radical towards the benzyl cation **D** and $\cdot OH$. Next, the deprotonation of benzoic acid by $\cdot OH$ gave the benzoate anion **E**. In path II, the attraction between **D** with **E** led to product **3**. In 2018, Xiong and co-workers extended the phosphorylation of the $C(sp^3)$ -H bonds of methyl-substituted arenes **19** with diaryl phosphinic acids **18** via Bu_4NI -catalyzed dehydrogenative coupling for the synthesis of organophosphorus compounds **20** in moderate to excellent yields (42–98%) (Scheme 10).²⁵ Toluene bearing electron-donating groups or halogens showed a higher reactivity than that of the toluene with electron-withdrawing groups. The screening of catalysts and oxidants showed that Bu_4NI and TBHP have the best effectivity. Bu_4NBr , 18-crown-6-ether and I_2 did not have any catalytic activity. For oxidants, TBPB and $K_2S_2O_8$ led to low yields (26–36%), and DTBP, H_2O_2 , *m*-CPBA and $H_3K_5O_18S_4$ were not workable.

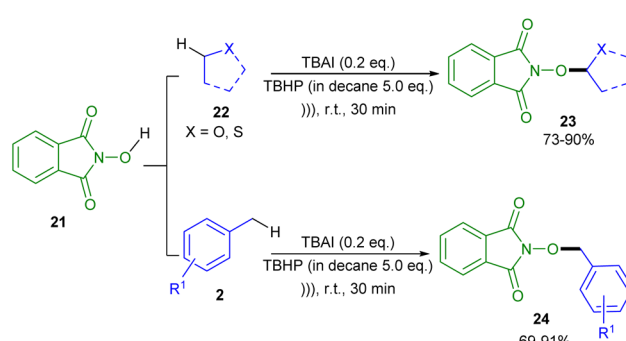
In 2019, Gui and co-workers succeeded in synthesizing *O*-alkylated hydroximides **23–24** under metal and solvent-free conditions with ultrasound acceleration (40 kHz/40 W) (Scheme 11).²⁶ The coupling reaction occurred between *N*-hydroxyphthalimide **21** (NHPI) and toluene **2**, or ether/thioether compounds **22**. The ultrasound technique can enhance the efficiency and rate of the reaction and minimize the side reactions. The screening of other oxidants such as H_2O_2 or $Na_2S_2O_8$ was not effective for this coupling reaction. The reaction proceeded through a radical mechanism, which was initiated with the generation of *tert*-butoxyl and *tert*-butylperoxy radicals from the decomposition of TBHP under iodide ion catalysis. These radicals then trapped a hydrogen atom from NHPI to form the phthalimide *N*-oxyl (PINO) radical **A**. The PINO radicals abstracted a benzylic or etheric hydrogen atom from **2** or **22** to produce the carbon radical **B**. The formation of these new stable



Scheme 8 Direct oxidative esterification of benzylic hydrocarbons with carboxylic acids (Liu and co-workers).²⁴

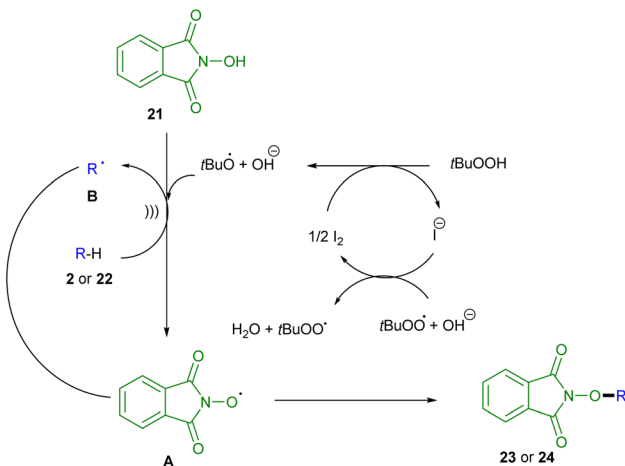


Scheme 9 Tentative mechanism for the oxidative esterification of benzylic hydrocarbons with carboxylic acids.



Scheme 11 Synthesis of *N*-alkoxyphthalimides through ultrasound acceleration (Gui and co-workers).²⁶





Scheme 12 Possible mechanism for the synthesis of *N*-alkoxyphthalimides through ultrasound acceleration.

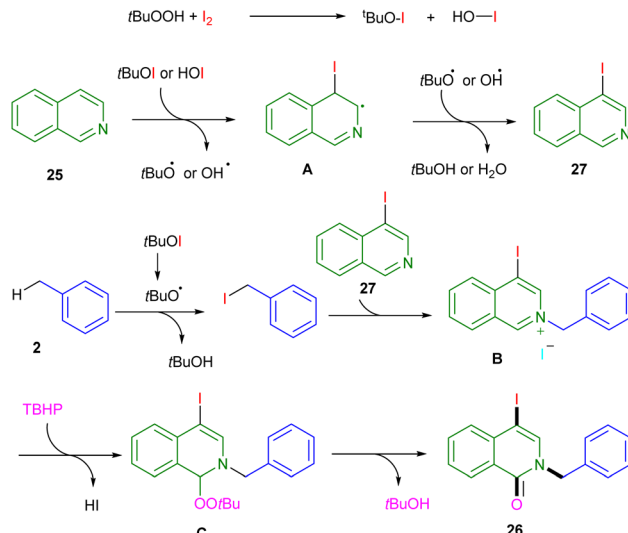
carbon radicals was promoted by ultrasonic radiation, which was then reacted with PINO radical **A** to yield product **23** or **24** (Scheme 12).

The I_2 /TBHP catalytic system can be utilized for the cross-coupling reaction of isoquinolines **25** with toluene derivatives **2** (Scheme 13).²⁷ In this method, various iodoisoquinolinones **26** were obtained *via* sequential $C(sp^2)$ -iodination/*N*-benzylolation/amidation reactions. TBHP as an initiator reacted with I_2 to produce *t*BuOI and HOI. The attack of these radicals on the C4 site of isoquinoline **25** provides radical intermediate **A**. The rearomatization of **A** yielded 4-iodoisooquinoline **27** through direct hydrogen abstraction or oxidation to the carbon cation and deprotonation. Meantime, the benzylic $C(sp^3)$ -H bond iodination of **25** occurred *via* the attack of *t*BuOI to generate benzyl iodide, followed by the reaction with **27** to give quaternary ammonium salt **B**. The nucleophilic addition of TBHP, followed by the removal of a *t*BuOH molecule, yielded *N*-benzyl-4-iodoisooquinolin-1(2*H*)-ones **26** (Scheme 14). It should be noted that the use of quinoline as a coupling partner afforded *N*-benzyl-3-iodoisooquinolin-2(1*H*)-ones.

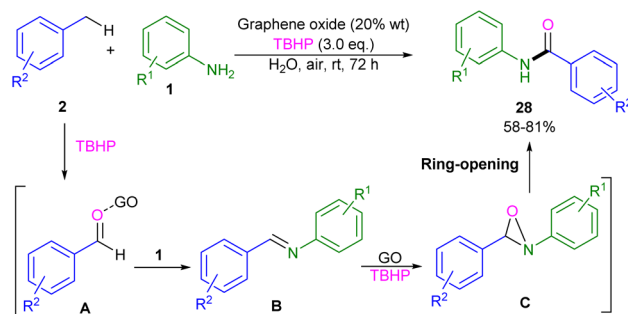
Graphene oxide in combination with TBHP can catalyze $C(sp^3)$ -H activation/amidation of toluene derivatives **2** (Scheme 15).²⁸ The method featured metal-free, base-free and ligand-free synthesis of amides, the use of green solvent H_2O , room-temperature reaction and recyclability of graphene oxide. First, TBHP promoted the oxidation of toluene to benzaldehyde. The acidic groups on the surface of graphene oxide can activate



Scheme 13 Reaction of isoquinolines and toluene derivatives via iodination/*N*-benzylation/amidation sequence (Yang and co-workers).²⁷



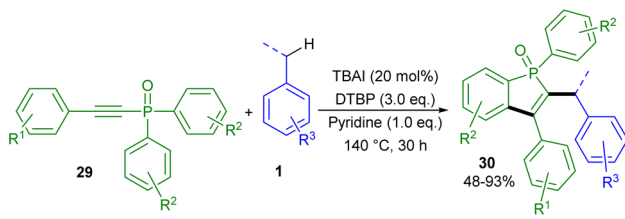
Scheme 14 Plausible mechanism for the reaction of isoquinolines and toluene derivatives *via* the iodination/*N*-benzylation/amidation sequence.



Scheme 15 Graphene oxide/TBHP-catalyzed reaction toluene with aniline (Dandia and co-workers).²⁸

the carbonyl of benzaldehyde **A** and facilitate the attack of the amine nucleophile to form the imine intermediate **B**. Afterwards, TBHP oxidized the imine to the oxaziridine intermediate **C**, which under thermal rearrangement, followed by the migration of a hydrogen placed *trans* to the nitrogen lone pair, furnished amide **28**. The evaluation of other carboxylic acid catalysts was not as effective as graphene oxide. When *o*-phenylenediamine was used as the substrate in the reaction with a toluene derivative, 2-aryl-1*H*-benzimidazoles was obtained *via* the intramolecular nucleophilic cyclization of the imine intermediate.

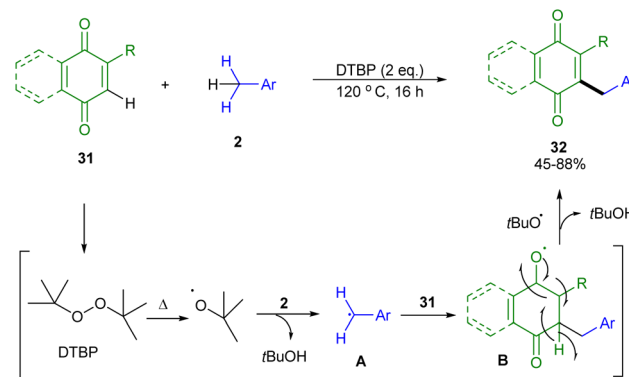
2.1.2. $C(sp^3)$ -H functionalization using DTBP. In 2016, the Gao lab introduced a new method for the synthesis of benzo[*b*] phosphole compounds **30** using a TBAI/DTBP simple system for the radical addition/cyclization of diaryl(aryl ethynyl)phosphine oxides **29** with toluene derivatives **2** (Scheme 16).²⁹ TBAI served as a catalyst in this reaction. After screening of other catalysts such as KI, Bu_4NBr and Bu_4NCl , the authors found that KI also improved the efficiency. To confirm the reaction mechanism, the authors conducted kinetic isotope effect (KIE) experiments. Deuterated toluene was used, and a KH/KD value of 1.72 was



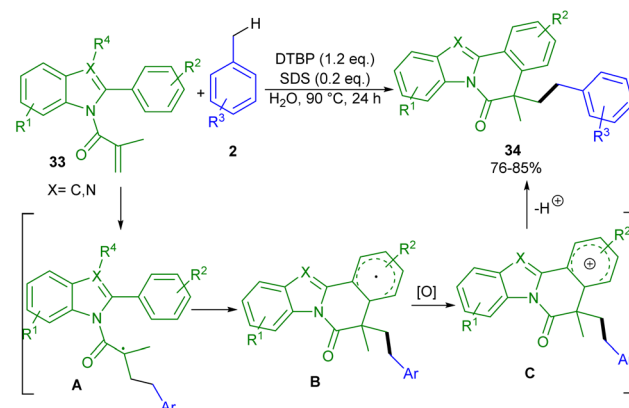
Scheme 16 TBAI-catalyzed radical addition/cyclization of diaryl(phenylethynyl)phosphine oxides with toluene derivatives (Gao and co-workers).²⁹

observed, indicating that the C–H bond cleavage on the methyl of toluene was not involved in the rate-limiting step. In addition, the use of 4.0 equivalents of BHT as a radical trapper stopped the transformation, indicating that the reaction occurred through the SET pathway. Thus, the authors propose a radical mechanism outlined in Scheme 17. At first, the *tert*-butoxyl and *tert*-butylperoxy radicals were produced with the help of the iodide anion. The benzyl radical **A** was generated through the abstraction of hydrogen by these radicals from toluene. Next, the regioselective attachment of the carbon radical to the α -position of the P=O bond in **29** produced the alkenyl radical **B**. The author envisaged that radical **B** underwent two possible pathways to yield the expected product **30** based on the production of two regioisomeric products.

Cross-dehydrogenative coupling reaction of quinones and 1,4-naphthoquinones **31** with benzylic C–H bonds **2** can be efficiently promoted by DTBP (Scheme 18).³⁰ The corresponding products were obtained in moderate to high yields. Toluene with an electron-donating group such as Me and OMe can enhance the reaction efficiency, affording higher yields (75–88%), while electron-poor toluene bearing Br or Cl groups yielded 62–67%. The reaction also led to low yields in the presence of other organic peroxides, such as TBHP, TBPB and BPO. Although PhI(OAc)₂ resulted in a 46% chemical yield. Radical trapping experiments using TEMPO and BHT suggested a radical route, in which the generated benzylic radical **A** by DTBP attacked the electron-deficient olefinic bond of quinone



Scheme 18 DTBP-mediated cross-coupling of quinones with benzylic C(sp³)-H bonds (Wang and co-workers).³⁰

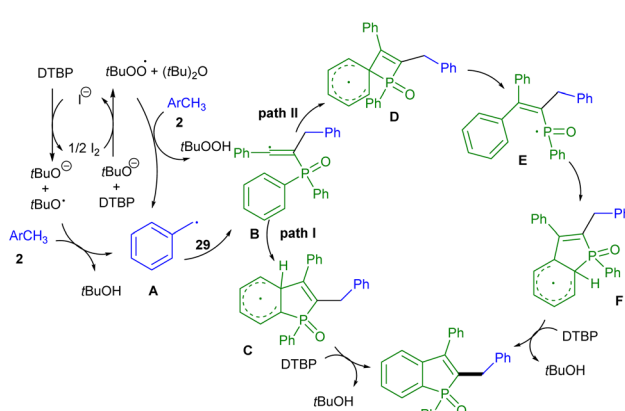


Scheme 19 DTBP-promoted radical cyclization of 2-arylbenzimidazoles with toluene (Wei and co-workers).³¹

31 to generate an oxygen radical **B**, followed by losing a hydrogen atom by peroxide.

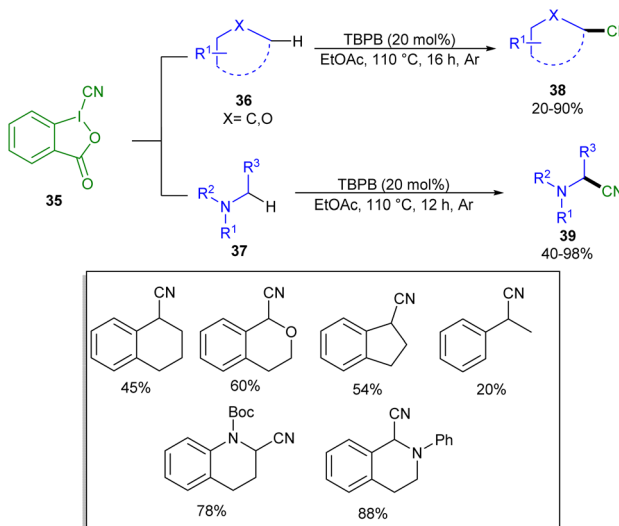
DTBP-promoted radical cyclization of 2-arylbenzimidazoles **33** with toluene **2** and unactivated alkanes was reported by Liu and Wei *et al.* in 2022 (Scheme 19).³¹ A wide range of benzimidazo[2,1-*a*]isoquinolin-6(5*H*)-one scaffolds were constructed in high yields from both toluene derivatives and unactivated alkanes. The reaction was conducted in water as the solvent, and sodium dodecyl sulfate (SDS) was used as a phase transfer agent. The use of TEMPO, BHT and 1,1-diphenylethene (DPE) as radical scavengers demonstrated that a radical pathway is involved, in which the unactivated C(sp³)-H bond was broken under the action of *tert*-butoxyl radical, producing a carbon radical, which attacked the alkene moiety in substrate **33** to form alkyl radical **B**, and then aryl radical **C**. The oxidation of **B** to **C** and subsequent oxidation of **C** delivered product **34**.

2.1.3. C(sp³)-H functionalization using TBPB. In 2018, a transition metal-free direct C(sp³)-H cyanation reaction between a wide range of substrates such as alkanes, ethers and tertiary amines with cyanobenziodoxolones was described by Zhang and co-workers (Scheme 20).³² In this reaction, cyanobenziodoxolone served as both a cyanating agent and oxidant. The cyanation reactions can proceed *via* two plausible



Scheme 17 Possible mechanism for the radical addition/cyclization of diphenyl(phenylethynyl)phosphine oxide with toluene.

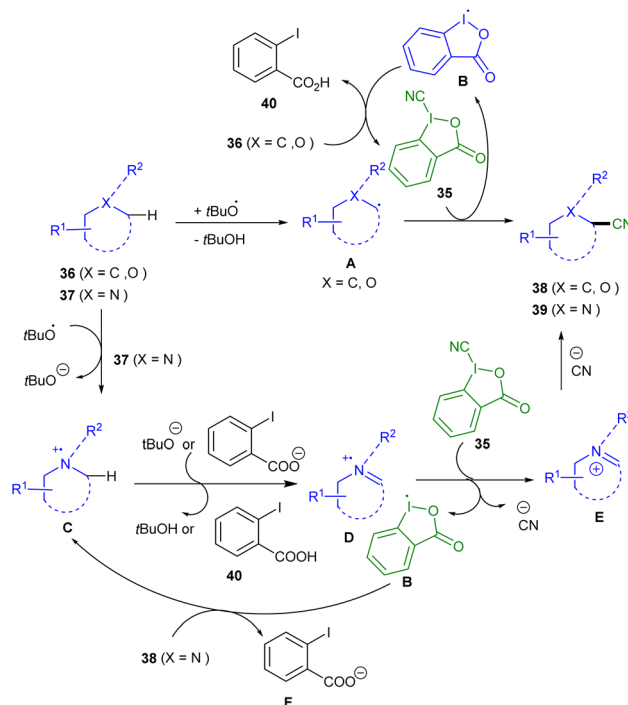




Scheme 20 TBPB-promoted $C(sp^3)$ -H cyanation between alkanes, ethers and tertiary amines with cyanobenziodoxolones (Zhang and co-workers).³²

mechanisms depending on the structure of the substrates: (i) a free radical pathway for alkanes and ethers and (ii) an oxidative pathway for tertiary amines. Path I (for alkanes and ethers) represented a free radical route for the cyanation of alkanes and ethers, which began with the generation of the radical $t\text{BuO}^\cdot$ from TBPB as an initiator. Then, $t\text{BuO}^\cdot$ extracted a hydrogen atom from the R-H bond of the substrate to generate carbon radical A, followed by the interaction with 35 to yield nitrile 38 and an iodine-centered radical B. Another hydrogen abstraction from the substrate was performed by the reactive radical B to yield 2-iodobenzoic acid 40 and A. Meantime, the cyanation of A yielded product 38 or 39. In the case of tertiary amines (path II), after the generation of $t\text{BuO}^\cdot$, a single electron transfer (SET) from the nitrogen atom of amine to $t\text{BuO}^\cdot$ gave N-centered cation radical C and a *tert*-butoxy anion ($t\text{BuO}^\cdot$). Then, C was deprotonated to the α - $C(sp^3)$ radical D, followed by SET oxidation by 35 to obtain iminium cation E along with the release of B and a cyanide anion. Nucleophilic attack of cyanide anion to E delivered the nitrile product 40. However, C was regenerated *via* the SET oxidation of substrate 38 with B (Scheme 21).

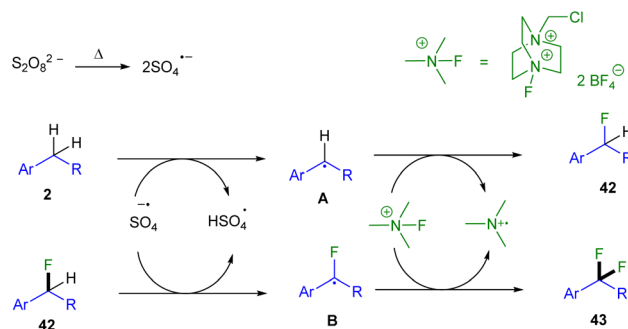
2.1.4. $C(sp^3)$ -H functionalization using $K_2S_2O_8$. In 2015, $K_2S_2O_8$, an inorganic oxidant, was used as an initiator in the coupling reaction between toluene derivatives and Selectfluor (Scheme 22).³³ Mono- and di-fluorination of the benzylic $C(sp^3)$ -H bond was carried out in this method. The radical mechanism involved the formation of a SO_4^\cdot anion radical from $K_2S_2O_8$, followed by the attack on the benzylic hydrogen of 2. The generated benzylic radical A captured a fluorine atom from 41 to form the monofluorinated compound 42. However, difluorinated arene 43 was obtained *via* the abstraction of another fluorine atom by fluorinated benzylic radical B (Scheme 23). In 2017, a similar reaction condition was used for the $C(sp^3)$ - $C(sp^3)$ homocoupling of toluene (Scheme 24).³⁴ The screening of



Scheme 21 Plausible pathways for the $C(sp^3)$ -H cyanation of alkanes, ethers and tertiary amines with cyanobenziodoxolones.

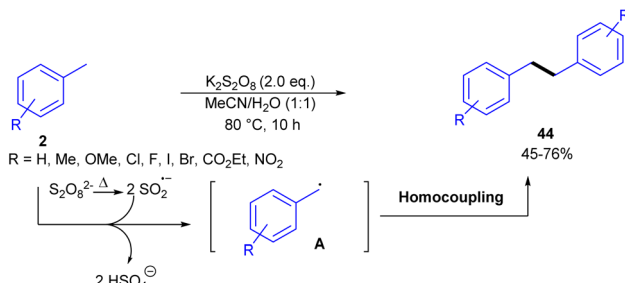


Scheme 22 $K_2S_2O_8$ -promoted selective benzylic mono- and di-fluorination (Yi and co-workers).³³



Scheme 23 Proposed mechanism for $K_2S_2O_8$ -promoted selective benzylic mono- and di-fluorination.

various organic and inorganic peroxides showed that only inorganic peroxides such as $\text{Na}_2\text{S}_2\text{O}_8$, $(\text{NH}_4)_2\text{S}_2\text{O}_8$ and $K_2\text{S}_2\text{O}_8$ were workable, and the best result was obtained using 2 equiv. of $K_2\text{S}_2\text{O}_8$ in a mixture of CH_3CN and H_2O as the reaction solvent at 80°C . A cross-coupling reaction between toluene and 1-methylnaphthalene was also carried out leading to 25% yield.

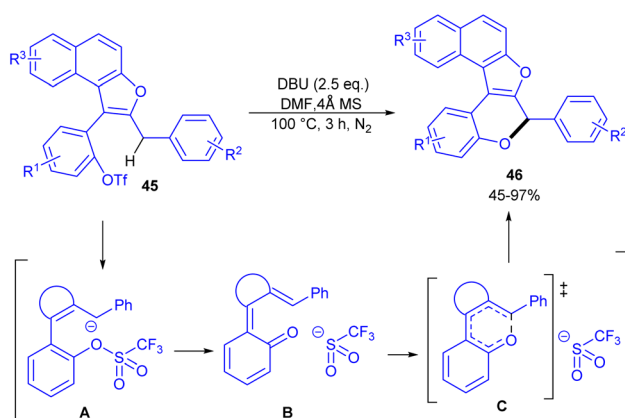


Scheme 24 $\text{K}_2\text{S}_2\text{O}_8$ -promoted homocoupling of toluene (Singh and co-workers).³⁴

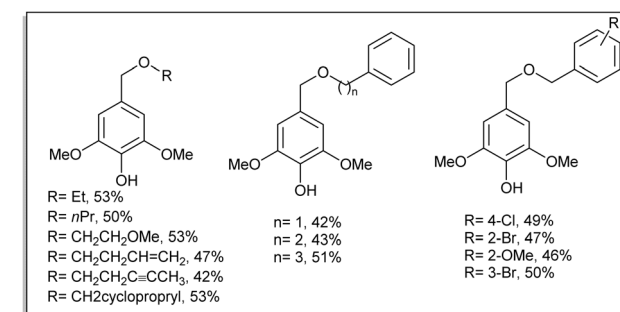
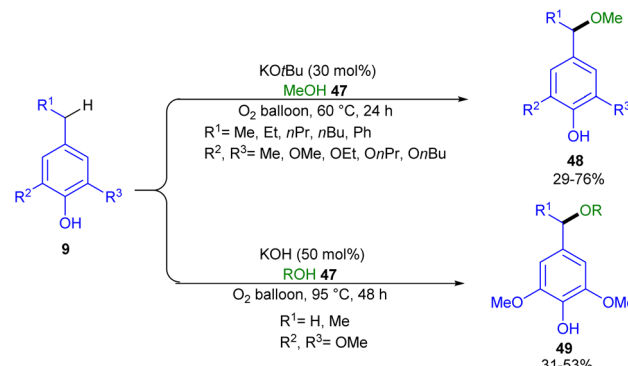
The radical trapping experiment using TEMPO suggested a radical route, which started with the thermal decomposition of $\text{K}_2\text{S}_2\text{O}_8$ to $\text{SO}_4^{\cdot-}$, followed by the trapping of methylarene 2 by this anion radical to generate a benzyl radical A. The dimerization of A delivered the dibenzyl product 44.

2.2. $\text{C}(\text{sp}^3)\text{-H}$ functionalization using bases

C-H activation/intramolecular annulation reaction towards the synthesis of helical chromenes was reported by He and Kwong *et al.* in 2022 (Scheme 25).³⁵ This metal-free ring-closure strategy showed moderate to good product yields and good functional group compatibility, particularly for the challenging Br and Cl groups. The reaction was proposed to proceed through either a radical mechanism or an anion mechanism. Mechanistic and DFT studies demonstrated that quinone is a key intermediate, which was generated from an anionic intermediate A. In the comparison between the radical and anionic pathways, the possible intermediates in the ionic pathway exhibit lower activation energy and more stability than the radical pathway. Therefore, a stepwise mechanism starting from anionic intermediate A was proposed, which started with the removal of the triflate group, leading to a stable quinone intermediate B. Next, oxa-6 π -electrocyclization through transition state C provided product 46.

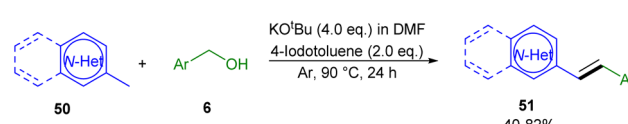


Scheme 25 Redox-neutral benzyllic C-O cyclization generating helical chromenes (He and co-workers).³⁵



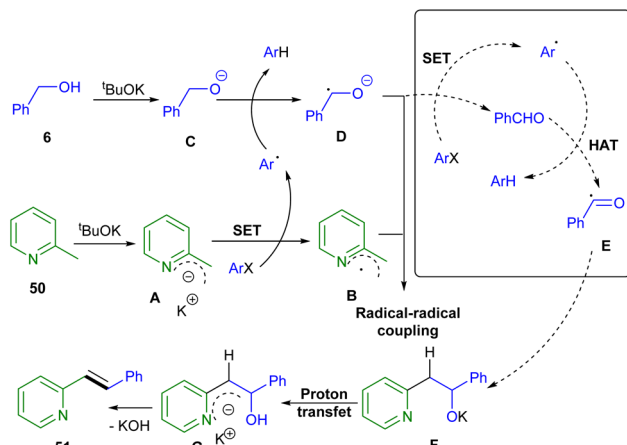
Scheme 26 Redox-neutral benzyllic C-O cyclization generating helical chromenes (Li and co-workers).³⁶

In 2024, a new metal-free base-catalyzed C-H functionalization reaction of toluene derivatives 9 was introduced by Li and colleagues (Scheme 26).³⁶ Two bases, namely KOtBu and KOH, were employed to catalyze the cross-dehydrogenative coupling reaction between benzyllic $\text{C}(\text{sp}^3)\text{-H}$ bonds and alcohols using molecular oxygen as a green oxidant. Given that KOtBu is a stronger base, the C-H activation reactions in the presence of this base can be carried out under milder conditions (less equiv. of the base compared to KOH, lower temperature and shorter reaction time). In addition, a wide range of aliphatic, benzyllic and cyclic alcohols participated smoothly in the alkoxylation of the primary and even secondary benzyllic C-H bonds of toluene. In the same year, another KOtBu-promoted $\text{C}(\text{sp}^3)\text{-C}(\text{sp}^3)$ cross-coupling between methyl N-heteroarenes 50 and benzyllic alcohols 6 was reported (Scheme 27).³⁷ Based on DFT calculations, a SET/HAT mechanism was suggested, in which anion A was produced in the presence of KOtBu. After that, the SET reduction in the aryl halide additive afforded an aryl radical and deprotonated methyl N-heteroarene A to produce radical B. However, the HAT process between alcoholate C from benzyllic alcohol 6 and the aryl radical gave the alcohol anion radical D



Scheme 27 KOtBu-promoted $\text{C}(\text{sp}^3)\text{-C}(\text{sp}^3)$ cross-coupling between methyl N-heteroarenes and benzyllic alcohols (Taillefer and co-workers).³⁷

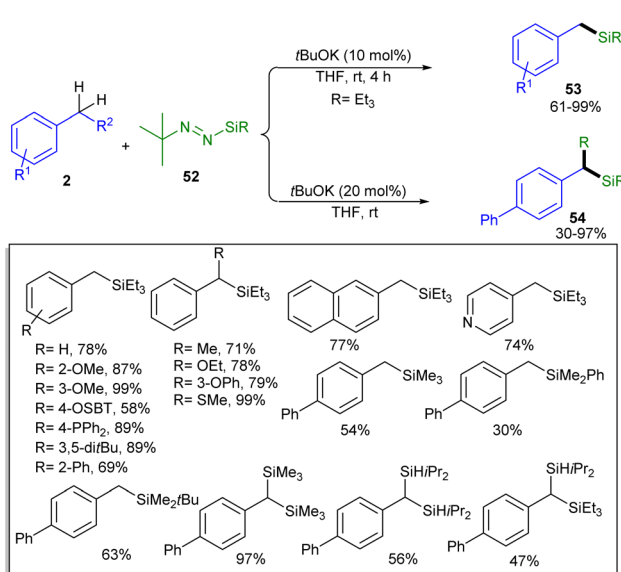




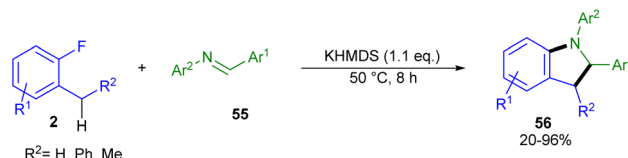
Scheme 28 Possible mechanism for the KOTBu -promoted $\text{C}(\text{sp}^3)$ - $\text{C}(\text{sp}^3)$ cross-coupling between methyl N-heteroarenes and benzylic alcohols.

and ArH . The radical–radical coupling of **B** and **D** provided intermediate **F**, followed by a proton transfer and subsequent elimination of KOH to yield olefin **51** (Scheme 28). KOTBu can also catalyze the silylation of benzylic $\text{C}(\text{sp}^3)$ -H bonds **2** using stable *tert*-butyl-substituted silyldiazene ($t\text{Bu}-\text{N}=\text{N}-\text{SiR}_3$) **52** as the silicon source (Scheme 29).³⁸ The protocol featured high and selective catalytic activity of KOTBu in combination with $t\text{Bu}-\text{N}=\text{N}-\text{SiR}_3$ towards the formation of $t\text{BuK}$ that further moved through an anionic chain process for the silylation of benzylic C–H bonds, leading to various mono- or *gem*-bis benzyl(di)silanes **53**–**54**. The replacement of KOTBu with $n\text{BuLi}$, KOH , NaOTBu or Me_3SiOK led to a lower yield of products (7–82%).

In 2024, potassium hexamethyldisilazide (KHMDS) was employed for constructing 1,2-diaryl-2,3-dihydroindoles **56** from *ortho*-fluorinated methyl-arenes **2** and *N*-aryl imines **55**



Scheme 29 KOTBu -catalyzed silylation of benzylic $\text{C}(\text{sp}^3)$ -H bonds (Chauvier and co-workers).³⁸



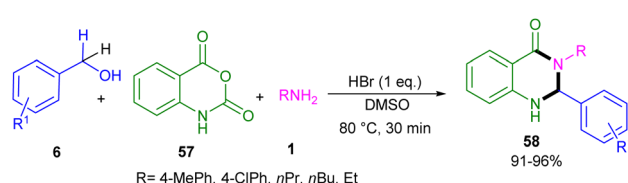
Scheme 30 KHMDS-promoted reaction of *ortho*-fluorinated methyl-arenes and *N*-aryl imines (Hintermann and Weindl).³⁹

under solvent-free conditions (Scheme 30).³⁹ The method proceeded through the benzylic $\text{C}(\text{sp}^3)$ -H activation *via* the deprotonation by the base, intermolecular 1,2-addition of the benzylic carbanion to the imine, and subsequent defluorinative $\text{S}_{\text{N}}\text{Ar}$ -annulation. The synthesis of a wide variety of indolines was performed without the need for any metal catalyst, and only 1.1 equiv. of KHMDS was found to be sufficient, as its strong basic ability allowed the reaction to occur under mild conditions. Other weaker alkali metals such as Li and Na were not effective.

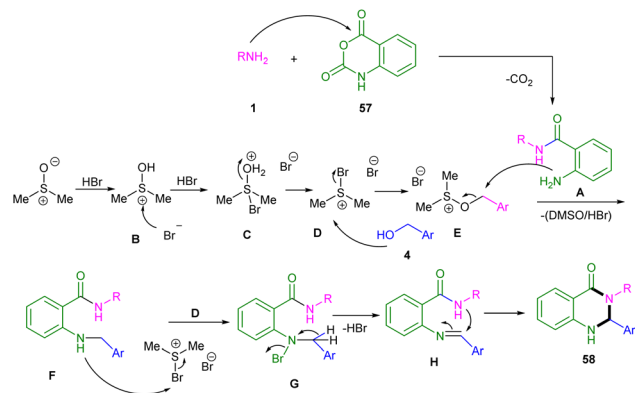
2.3. $\text{C}(\text{sp}^3)$ -H functionalization using acids

In 2018, Rashidi Ranjbar and co-workers developed a metal-free protocol for the synthesis of 2,3-dihydroquinazolin-4(1*H*)-one scaffolds (Scheme 31).⁴⁰ A three-component reaction, including aryl/alkylamines **1**, isatoic anhydride **57**, and arylalcohols **6** was designed in the presence of HBr and DMSO . Interestingly, bromodimethylsulfonium bromide (BDMS) intermediate **D** was generated *in situ* from HBr and DMSO under reaction conditions. This reactive intermediate was then subjected to the nucleophilic attack of alcohol to form the alkoxy sulfonium ion **E**. However, isatoic anhydride underwent ring-opening by the nucleophilic addition of amine to access anthranilamide **A**. Another nucleophilic attack of **E** occurred by anthranilamide **A** to obtain *N*-benzyl intermediate **F** by losing HBr and DMSO molecules. Then, the interaction of BDMS with **F** and subsequent HBr elimination afforded the imine intermediate **H**. The generated HBr in this step can react with DMSO to regenerate BDMS. Finally, intramolecular cyclization in **H** produced 2,3-dihydroquinazolin-4(1*H*)-ones **58** (Scheme 32). This method has the advantages of using alcohols instead of aldehydes or ketones in the reaction with anthranilamide, short reaction times and mild conditions.

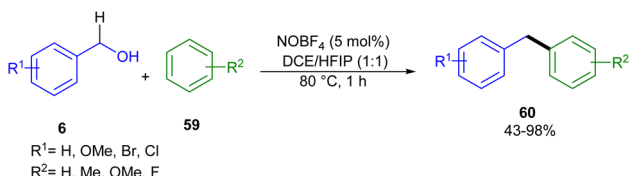
In the same year, Antonchick and his team developed a methodology for the $\text{C}(\text{sp}^3)$ -H arylation of benzyl alcohols **6** in the presence of a Lewis acid catalyst (Scheme 33).⁴¹ For this purpose, NOBF_4 (5 mol%) was served as a Lewis acid in



Scheme 31 Oxidative $\text{C}(\text{sp}^3)$ -N coupling using HBr and DMSO towards 2,3-dihydroquinazolin-4(1*H*)-ones (Rashidi Ranjbar and co-workers).⁴⁰



Scheme 32 Tentative mechanism for $C(sp^3)$ -N coupling using HBr and DMSO towards 2,3-dihydroquinazolin-4(1H)-ones.



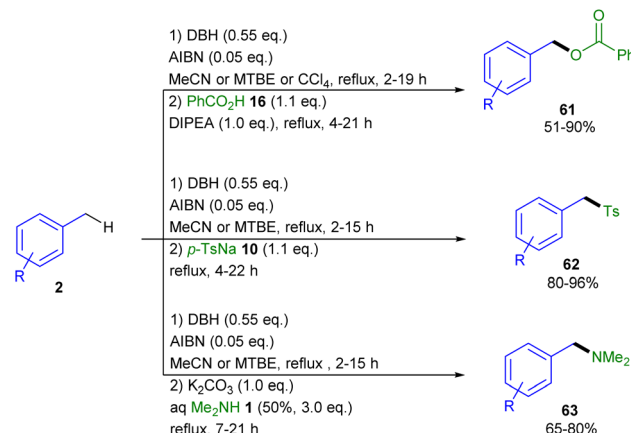
Scheme 33 Lewis acid-promoted arylation of benzyl alcohols (Antonchick and co-workers).⁴¹

a mixture of benzyl alcohols **6** and arenes **59**, in DCE/HFIP (1 : 1) at 80 °C. Various polysubstituted arenes reacted well with a wide range of electron-rich and electron-poor primary, secondary and tertiary benzyl alcohols. A range of diarylmethane derivatives were constructed in moderate to excellent yields (43–98%). They also used this catalytic system for the intramolecular rearrangement of benzyl phenyl ethers towards benzyl phenols.

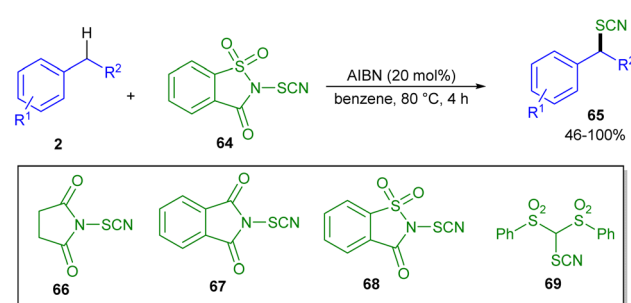
2.4. $C(sp^3)$ -H functionalization using other radical initiators

In 2015, Togo and co-workers reported the reaction of toluene derivatives **2** with nucleophiles under metal-free conditions (Scheme 34).⁴² For this purpose, various nucleophiles, such as benzoic acid **16**, sodium *p*-toluenesulfinate **10**, *p*-toluenethiol, aqueous dimethylamine **1**, and succinimide were treated with both electron-rich and electron-poor toluene in the presence of 1,3-dibromo-5,5-dimethylhydantoin (DBH) or *N*-bromosuccinimide (NBS) and a catalytic amount of 2,2'-azobis(isobutyronitrile) (AIBN) as a radical initiator. Sodium *p*-toluenesulfinate gave higher yields (80–96%) than those of other nucleophiles. The reaction proceeded through a one-pot two-step process, where in the first step, the generated benzyl radical, with the assistance of AIBN and DBH, coupled with radical bromine to obtain benzyl bromide. In the next step, the nucleophile attacked the C-Br bond to produce the desired product.

In 2021, AIBN was utilized as an initiator for the thiocyanation of toluene derivatives (Scheme 35).⁴³ Several thiocyanating reagents were evaluated in the reaction with toluene, in which **64** showed better efficiency among others. It seems that the SO₂ group plays an important role in the reactivity of **64** relative to



Scheme 34 Metal-free formation of C–O, C–S, and C–N bonds at the benzylic position of toluene (Togo and co-workers).⁴²

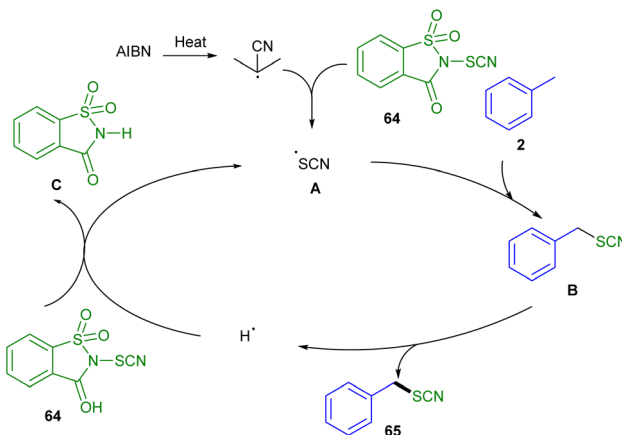


Scheme 35 $C(sp^3)$ -H thiocyanation of toluene in the presence of AIBN (Chen and co-workers).⁴³

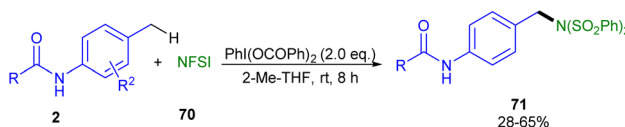
66 and **65**. Moreover, the undesired electrophilic substitution takes place on the phenyl ring of **69**. In general, electron-rich toluene derivatives gave higher chemical yields than those of electron-deficient ones. The radical trapping and mechanistic experiments revealed the presence of hydrogen and thiocyanato radicals **B** but no benzyl radical. The decomposition of AIBN to *tert*-butyl radical under heating and subsequent N-SCN cleavage gave SCN radical **A**. For showing the plausible mechanism, the authors used allylbenzene as a substrate, which underwent the addition of radical **A** to form intermediate **B**. The release of a hydrogen radical from **B** afforded the final product **65**. The generated hydrogen radical can react with **64** to form a SCN radical **A** for the next catalytic cycle (Scheme 36).

In 2018, benzylic C–H amination of methylarenes **2** with *N*-fluorobenzenesulfonimide (NFSI) **70** in the presence of a hypervalent iodine agent like PhI(OCOPh)₂ was reported by Li *et al.* (Scheme 37).⁴⁴ A series of 4-methylanilides, even multi-substituted 4-methylanilides, participated in this regioselective $C(sp^3)$ -H activation. A plausible mechanism was suggested by the authors, which started with the oxidation of 4-methylanilide **2** by the iodine(III) reagent to produce radical **A**. Then, through an SET, cation **B** was obtained from **A**, which could be due to isomerization with dienimine **C**. Meantime, NFSI was converted into the nitrogen radical, which then reacted with **C** to yield intermediate **D**. Finally, product **71** was



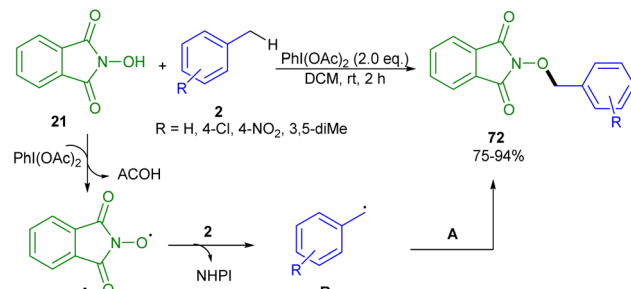


Scheme 36 Plausible mechanism for the $C(sp^3)$ -H thiocyanation of toluene in the presence of AIBN.

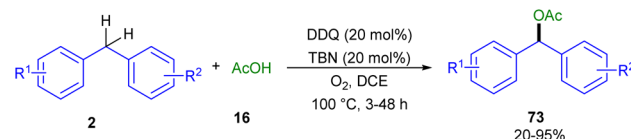


Scheme 37 Oxidative benzylic C-H amination of 4-methylanilides with *N*-fluorobenzenesulfonimide (Li and co-workers).⁴⁴

obtained from the interaction of 2 with **D**. The desulfonylation of the final sulfonamide was also carried out by conc. H_2SO_4 to provide benzylic amine (Scheme 38). In another reaction, $PhI(OAc)_2$ was used as a safe radical initiator instead of TBHP in the coupling of *N*-hydroxypthalimide (NHPI) 21 and unactivated $C(sp^3)$ -H bonds 2 (Scheme 39).⁴⁵ In this work, toluene derivatives bearing CH_3 , NO_2 and Cl functional groups were incorporated in the C-O bond formation with NHPI, yielding the corresponding products 72 in 75–94% yield. Overall, the reaction proceeded *via* the attack of two radicals, PINO[·] A and R' **B**, which were generated in the presence of $PhI(OAc)_2$ under



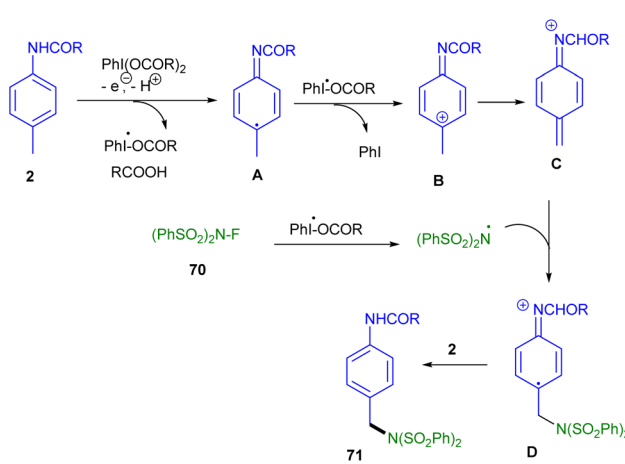
Scheme 39 Iodine(III)-promoted coupling of *N*-hydroxypthalimide (NHPI) with unactivated $C(sp^3)$ -H bonds (Wu and co-workers).⁴⁵



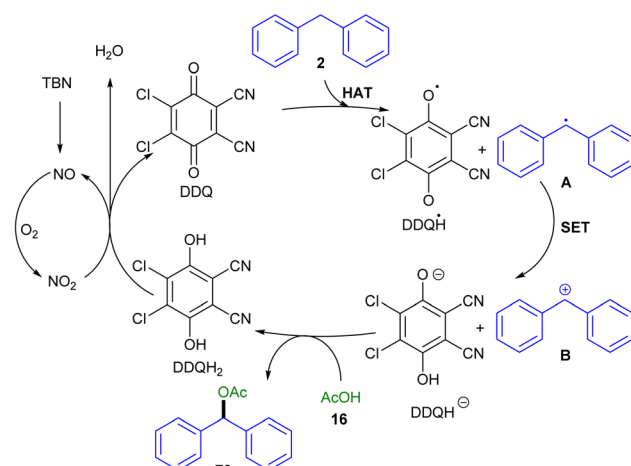
Scheme 40 Aerobic oxidative C-O coupling of $C(sp^3)$ -H with carboxylic acids (Li and co-workers).⁴⁶

heating. In addition to toluene, various alkanes, ethers, thioethers and nitriles were well tolerated in this mild coupling reaction.

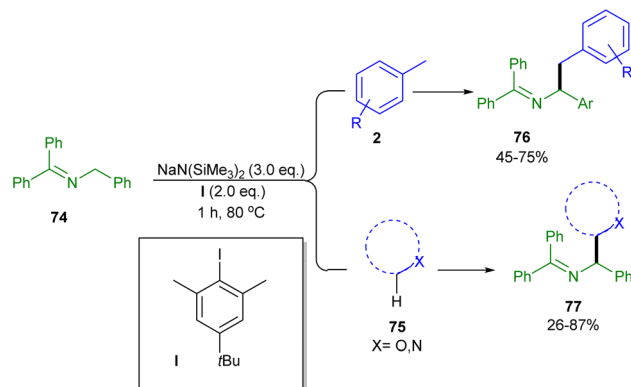
Acetoxylation of benzylic $C(sp^3)$ -H bonds was performed in the presence of 2,3-dichloro-5,6-dicyano-1,4-benzoquinone (DDQ) as a main catalyst and *tert*-butyl nitrite (TBN) as a co-catalyst (Scheme 40).⁴⁶ Aliphatic and aromatic carboxylic acids 16 can be incorporated in the reaction with diarylmethanes 2. The reaction could be influenced by the electronic effects of the functional groups on the aryl rings of substrate 2. The process involved a radical pathway according to the radical trapping experiment. First, TBN was converted into NO_2 under aerobic conditions. HAT between DDQ and 2 generated alkyl radical **A** and $DDQH$. Further, through a SET process, diphenylmethyl cation **B** and $DDQH^-$ were generated. Then, cation **B** reacted with



Scheme 38 Possible mechanism for the oxidative benzylic C-H amination of 4-methylanilides with *N*-fluorobenzenesulfonimide.



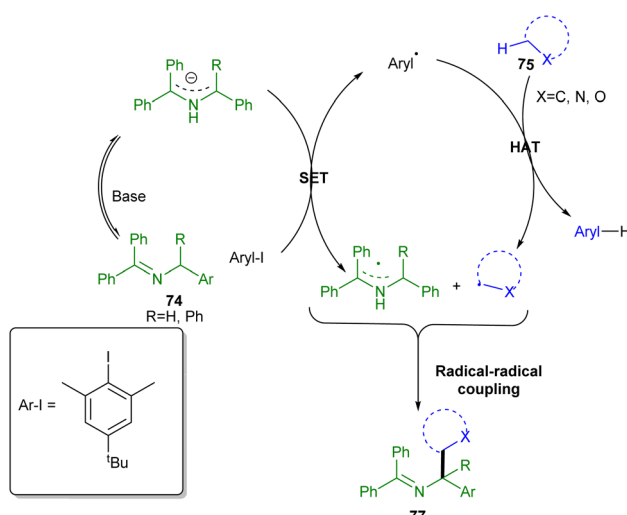
Scheme 41 Possible mechanism for aerobic oxidative C-O coupling of $C(sp^3)$ -H with carboxylic acids.



Scheme 42 $\text{C}(\text{sp}^3)\text{-H}/\text{C}(\text{sp}^3)\text{-H}$ dehydrogenative coupling of saturated heterocycles and toluene with *N*-benzyl imines (Zhang and co-workers).⁴⁷

carboxylic acid **16** to deliver acetoxylated product **73**. However, DDQH^- was protonated to DDQH_2 , which could be re-oxidized to DDQ by NO_2 (Scheme 41).

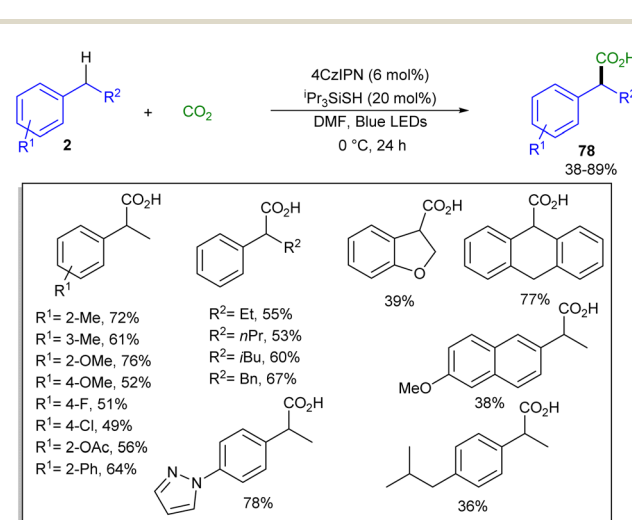
$\text{NaN}(\text{SiMe}_3)_2$ or $\text{LiN}(\text{SiMe}_3)_2$ with an aryl iodide can catalyze the C–C coupling between heterocyclic $\text{C}(\text{sp}^3)\text{-H}$ bonds and alkyl/benzyl $\text{C}(\text{sp}^3)\text{-H}$ bonds (Scheme 42).⁴⁷ However, $\text{KN}(\text{SiMe}_3)_2$ resulted in a mixture of products. $\text{NaN}(\text{SiMe}_3)_2$ was chosen as a better catalyst for the reaction of ketamine with toluene or saturated heterocycles with a C–H bond active. Unlike other $\text{C}(\text{sp}^3)\text{-H}$ activation reactions mediated by photoredox catalysts or peroxides, this reaction is based on the organic super electron donor (SED), 2-azaallyl anions. The reaction proceeded through the SET of 2-azaallyl anions and aryl iodides as electron acceptors, affording the aryl radical. Through a HAT process from toluene or saturated heterocycles to this aryl radical, a benzyl radical or alkyl radical was obtained, respectively. Coupling of the active radicals resulted in the formation of the target product **77** (Scheme 43).



Scheme 43 Plausible mechanism of $\text{C}(\text{sp}^3)\text{-H}/\text{C}(\text{sp}^3)\text{-H}$ dehydrogenative coupling of saturated heterocycles and toluene with *N*-benzyl imines.

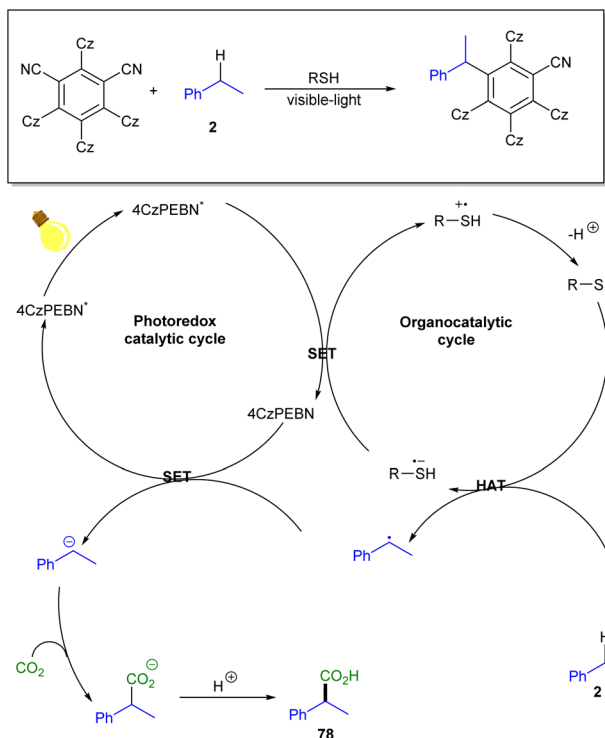
2.5. $\text{C}(\text{sp}^3)\text{-H}$ functionalization using visible light irradiation

In 2019, a facile method was introduced for the carboxylation of the benzylic $\text{C}(\text{sp}^3)\text{-H}$ bonds by applying synergistic effects between photoredox and organocatalysis (Scheme 44).⁴⁸ A diverse range of carboxylic acids were constructed using 4 atmospheric gaseous CO_2 under visible light conditions. The evidence of KIE study revealed that the C–H bond cleavage is involved in the rate-limiting step. Two catalytic cycles were involved in this transformation. In the photocatalytic cycle, 4CzPEBN^* was generated under visible light irradiation. In the meanwhile, RSH^+ ($\text{R} = \text{iPr}_3\text{Si}$) was formed from R-SH , which, in turn, was formed through a hydrogen atom transfer (HAT) process from alkylarene **2** and radical R-S^* in the organocatalytic cycle. The generated benzyl radical was then reacted with 4CzPEBN^* through another SET process to produce a benzyl anion intermediate. The addition of CO_2 to the benzylic C–H bond can form the corresponding carboxylic acid **78** after protonation. It should be noted that the process was carried out without the need for any sacrificial electron donor, electron acceptor or additives (Scheme 45). In 2024, the acylation of benzylic $\text{C}(\text{sp}^3)\text{-H}$ bonds **2** was established in the presence of 4CzIPN (Scheme 46).⁴⁹ Zhou *et al.* explored synergistic effects between the organophotocatalyst 4CzIPN and thiol for promoting the coupling reaction of toluene **2** and aromatic aldehydes **79**. In this method, a series of α -aryl ketones were synthesized through the formation of alcoholic species as a key intermediate, followed by acceptorless alcohol dehydrogenation. The reaction mechanism in details started with photoexcitation of 4CzIPN to the excited state 4CzIPN^* , followed by the interaction with thiol *via* SET to generate an electrophilic thiyl radical **A** after the deprotonation. A HAT process occurred between the $\text{C}(\text{sp}^3)\text{-H}$ bond of alkylarene and the thiyl radical **A** to render a benzyl radical **B**. Meanwhile, aldehyde was subjected to a proton-coupled electron transfer (PCET) with the reduced photocatalyst 4CzIPN^* to form the neutral ketyl

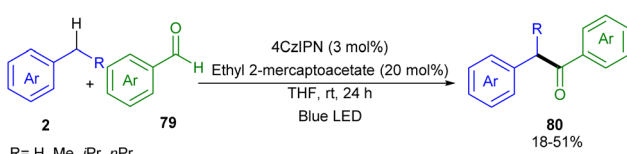


Scheme 44 Photocarboxylation of benzylic C–H bonds using CO_2 (König and co-workers).⁴⁸





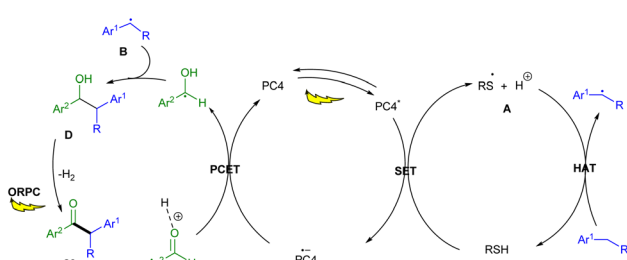
Scheme 45 Catalytic cycle for the photocarboxylation of benzylic C–H bonds using CO_2 .



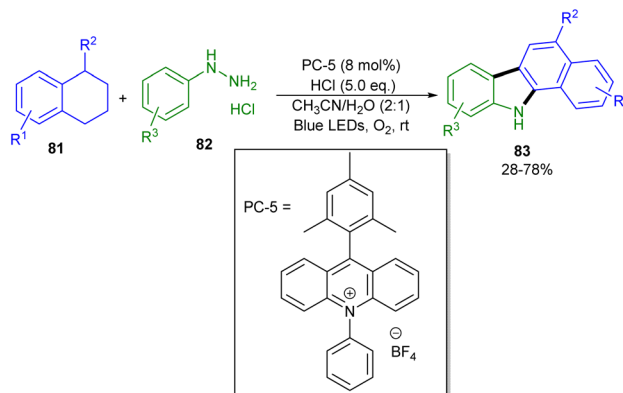
Scheme 46 Photocatalytic cross-coupling of the benzylic C–H bond of toluene with aromatic aldehydes (Guo and co-workers).⁴⁹

radical C. Next, benzylic radical B coupled with the ketyl radical C to provide the alcohol intermediate D, which through photocatalytic acceptorless dehydrogenation furnished ketone 80 (Scheme 47).

In 2019, Shen *et al.* explored a photoredox organocatalysis system for $\text{C}(\text{sp}^3)\text{–H}$ activation/annulation of tetrahydronaphthalene substrates 81, leading to benzo[a]carbazoles 83

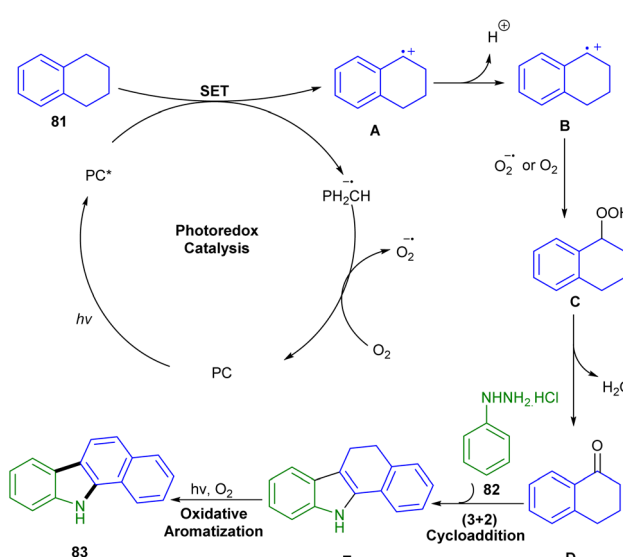


Scheme 47 Photocatalytic mechanism for the cross-coupling of the benzylic C–H bond of toluene with aromatic aldehydes.

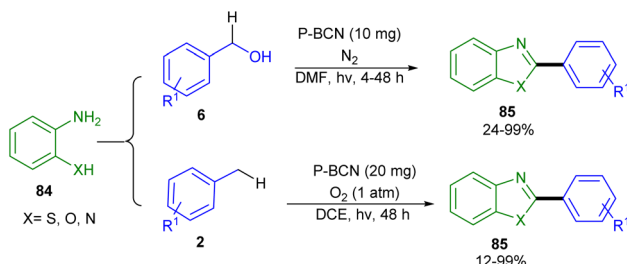


Scheme 48 $\text{C}(\text{sp}^3)\text{–H}$ activation/annulation of tetrahydronaphthalenes (Shen and co-workers).⁵⁰

(Scheme 48).⁵⁰ The authors employed 1,2,3,4-tetrahydronaphthalene and arylhydrazine hydrochlorides as starting materials in the presence of 10-phenyl-9-(2,4,6-trimethylphenyl) acridinium tetrafluoroborate as a photocatalyst under visible light conditions. Initially, the photocatalyst was converted into the excited-state catalyst under blue LEDs. Then, the excited-state species under a SET process with the benzylic $\text{C}(\text{sp}^3)\text{–H}$ bond afforded a radical cation A and a radical anion photocatalyst, which could be oxidized by O_2 in the ground-state photocatalyst. However, the radical cation A was converted to the radical B by losing a proton, followed by reaction with O_2 or the O_2 radical anion to yield the hydroperoxide C. Further dehydration of C afforded the ketone D, which underwent (3 + 2) cycloaddition with phenylhydrazine hydrochloride 82 to furnish 6,11-dihydro-5H-benzo[a]carbazole E. The oxidative aromatization of E resulted in the formation of benzo[a]carbazole 83 in the presence of O_2 (Scheme 49). Moreover, the large-scale synthesis of the product (0.6 g, 55%) showed the utility of this

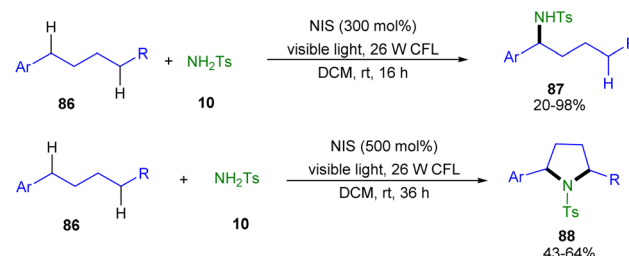


Scheme 49 Proposed mechanism for $\text{C}(\text{sp}^3)\text{–H}$ activation/annulation of tetrahydronaphthalenes.



Scheme 50 P-BCN-catalyzed alcohol oxidation/toluene $C(sp^3)$ -H activation with *o*-thio/hydroxy/aminoanilines (Jiang and co-workers).⁵¹

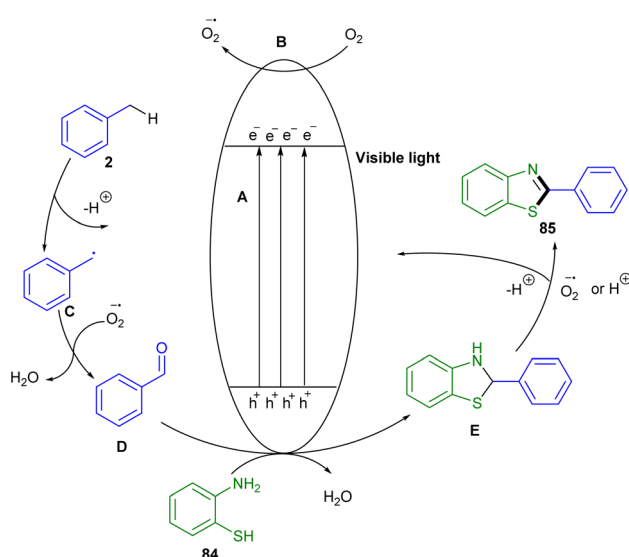
protocol. Another photocatalyst was used in the Jiang work for preparing benzothiazoles **85** from toluene **2** (Scheme 50).⁵¹ For this purpose, *o*-thio/hydroxy/aminoanilines **84** were used as coupling partners in the reaction with toluene **2** in the presence of porous borocarbonitride (P-BCN). Higher catalytic activity was observed using P-BCN compared to bulk BCN, which might be because of the crystallinity-enhancement-induced improvement in charge separation and transmission. This procedure features high substrate tolerance using a recyclable heterogeneous photocatalyst, water and O_2 as the green solvent and oxidant, respectively, which offers a sustainable and eco-friendly synthetic route. The overall mechanism involved the formation of electrons and holes **A** on the surface of P-BCN under blue-light irradiation. The O_2 oxidized to $O_2^{\cdot-}$ by the electrons on the conduction band **B**. In the case of holes, toluene was oxidized to benzaldehyde to form benzyl radical **C**, which was then oxidized and dehydrogenated by $O_2^{\cdot-}$ to form benzaldehyde **D**. The condensation of benzaldehyde with *o*-aminobenzenethiol **2** was promoted by the exposed **B** Lewis acid sites in P-BCN to generate 2,3-dihydrobenzothiazole **E**, followed



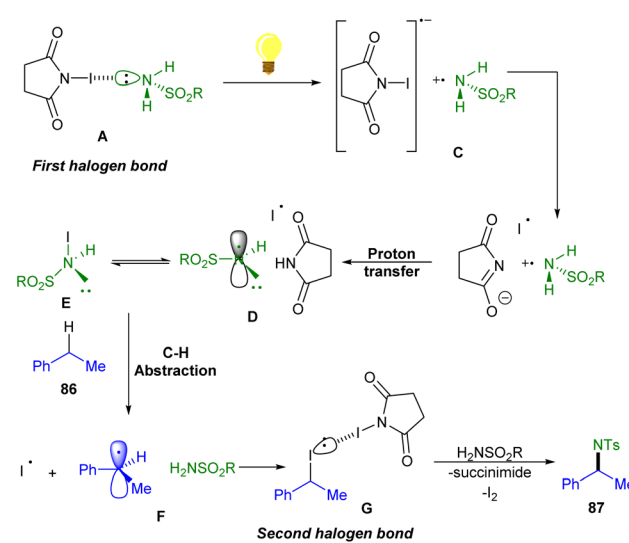
Scheme 52 $C(sp^3)$ -H activation/amination of arylalkyl substrates (Li and co-workers).⁵²

by oxidation to yield 2-phenylbenzothiazole **85** with the help of $O_2^{\cdot-}$ or photo-induced holes (Scheme 51).

Another visible light catalysis system was used for benzylic $C(sp^3)$ -H amination of various arylalkyl substrates **86** (Scheme 52).⁵² The KIE study showed that C-H activation is the rate-determining step. UV-vis studies demonstrated that the reaction did not occur without the irradiation. According to the mechanistic experiments, a rational mechanism was suggested for this procedure. Two different products can be synthesized *via* the $C(sp^3)$ -H activation of a diverse range of hydrocarbon substrates. When the reaction was carried out in the presence of 300 mol% of NIS as an initiator under visible light irradiation, benzylamines **87** were obtained after 16 hours, while increasing the amount of NIS to 500 mol% for 36 hours reaction time led to the formation of pyrrolidine products **88**. It seems that this reaction involved a HAT relay strategy to access pyrrolidine structures through two consecutive C-H bond aminations of alkanes with variable bond dissociation energies. According to the mechanism in Scheme 53, first, a halogen bond complex **A** initiated visible light absorption. The reaction mechanism involved photoexcitation and charge transfer towards a nitrogen-centered radical **D** and iodine, which could be in equilibrium with the N-I intermediate **E**. The abstraction of

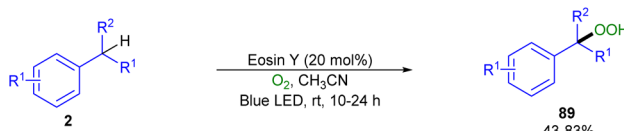


Scheme 51 Proposed mechanism for P-BCN-catalyzed alcohol oxidation/toluene $C(sp^3)$ -H activation with *o*-thio/hydroxy/aminoanilines.



Scheme 53 Possible mechanism for the $C(sp^3)$ -H activation/amination of arylalkyl substrates.

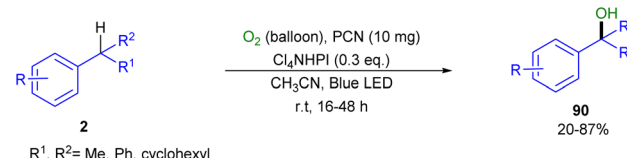




Scheme 54 Benzyl C(sp³)-H activation/hydroperoxidation using O₂ (Xing and co-workers).⁵³

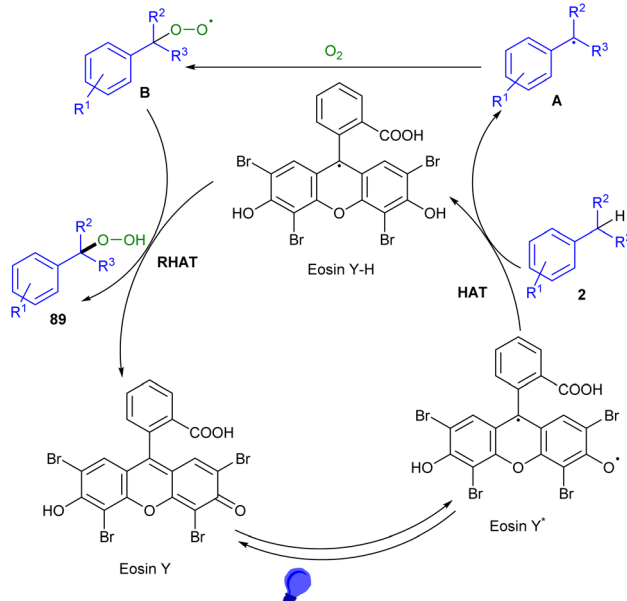
a hydrogen atom from the benzylic C-H bond by **D** gave radical **F**. The combination of the first iodide radical with **F**, followed by the second iodide bonding with NIS resulted in complex **G**. Finally, 1-iodoethylbenzene underwent the nucleophilic substitution of amine **10** to provide product **87**. A similar process was proposed for the subsequent Hofmann-Löffler-Freytag (HLF) reaction to produce pyrrolidine.

Benzyl C(sp³)-H activation/hydroperoxidation reaction can be carried out in the presence of O₂ catalyzed by a photoredox catalyst (Scheme 54).⁵³ In this context, Xing and co-workers utilized only 2 mol% of eosin Y photocatalyst to begin the reaction. After the excitation of the organocatalyst by light, alkylarene transferred a hydrogen atom to it to generate a benzyl radical **A**. This reactive carbon radical then underwent the addition of O₂ to obtain another active peroxy radical **B**. A retro-HAT between eosin Y-H and **B** resulted in the desired product **89** and the ground-state eosin Y. The catalyst can restart another catalytic cycle (Scheme 55). Many alkylarenes with different functional groups (OMe, I, Br, Cl, NO₂, COMe, and -C≡CH) were tolerated well, while heteroaromatics such as 2-ethyl thiophene, 2-alkyl pyridine and 3-alkyl indole were not feasible. Simple reaction conditions and avoiding any additives are the advantages of this work. Another research group used photocatalysis system for the hydroxylation of benzylic C-H bonds

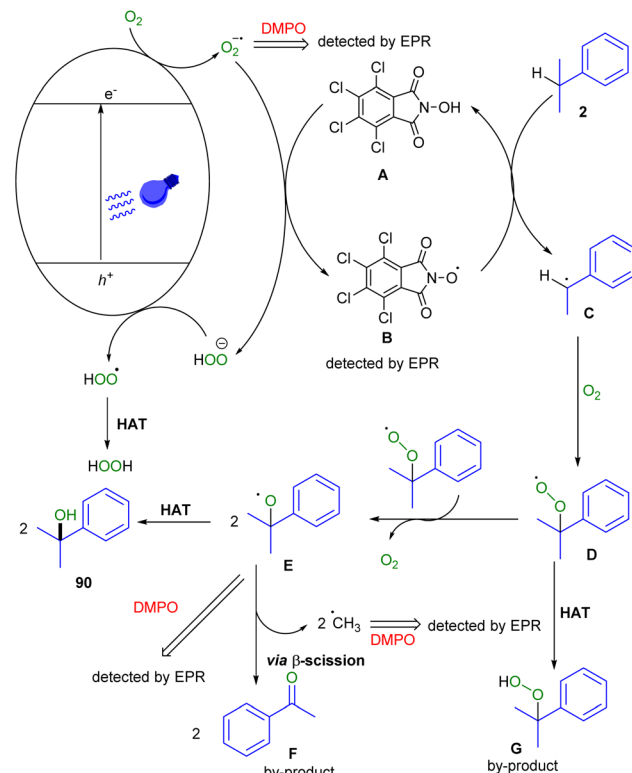


Scheme 56 Photocatalytic hydroxylation of benzylic C(sp³)-H bonds using O₂ (Das and co-workers).⁵⁴

using O₂ (Scheme 56).⁵⁴ In this work, tertiary alcohols can be constructed in good chemical yields. The mechanism involved the irradiation of visible light to activate the catalyst to the excited state, and to transform O₂ to O₂^{·-}. Then, the Cl₄PINO radical was also generated through a HAT process with O₂^{·-}, along with the formation of HOO[·] from O₂^{·-}. The oxidation of HOO[·] by photocatalysts and another HAT process provided H₂O₂. Next, the substrate was activated by the Cl₄PINO radical through another HAT process to render the cumyl radical **C**. In this step, cumene autoxidation *via* a free radical route occurred to form a cumyl radical, which further reacted with O₂ to produce the peroxy-intermediate **D**. Afterward, the dimethylbenzylalkoxyl radical **E** was generated *via* the reaction of two molecules of **D** with O₂. In addition, **D** gave the peroxide as a byproduct under the HAT process. Finally, **E** abstracted a hydrogen atom from the substrate to afford product **90** and restarted the chain reaction with **C** or underwent β -scission to furnish the acetophenone byproduct **F** (Scheme 57). Moreover,

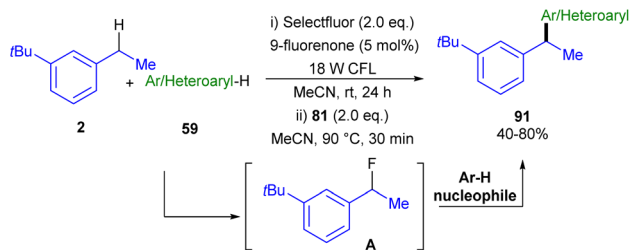


Scheme 55 Photocatalytic cycle for C(sp³)-H activation/hydroperoxidation using O₂.



Scheme 57 Catalytic cycle for the photocatalytic hydroxylation of benzylic C(sp³)-H bonds using O₂.



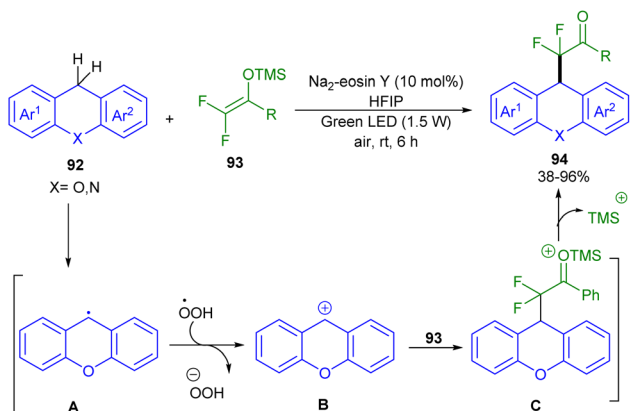


Scheme 58 Cross-dehydrogenative arylation of unactivated benzylic C–H bonds (Larrosa and co-workers).⁵⁵

the applicability of the method was shown with the recovery of the catalyst, the performance of the reaction under solar energy and the gram-scale synthesis of the product.

The Larrosa team described cross-dehydrogenative coupling between the benzylic C(sp³)–H bond of alkylarenes **2** and C(sp²)–H bond of aryl/heteroaryl compounds **59** (Scheme 58).⁵⁵ The method was proposed to be based on the formation of reactive benzyl fluoride intermediate **A** from the interaction of benzylic fluorination of alkylarene **2** using 9-fluorenone as a photocatalyst and selectfluor under visible light irradiation. This electrophilic intermediate then underwent S_EAr-type reaction with the nucleophilic aryl/heteroaryl coupling partners. It is noteworthy that the reaction of alkylarene with selectfluor can produce a benzylic electrophile containing a suitable leaving group that is recognized as a key intermediate for the reaction progress. This intermediate can easily react with nucleophiles without the need for an α -activating group and/or a *para* electron-donating group. The substitution occurred at the most electron-rich and less hindered position on the arene ring. As a result, a series of synthetically useful 1,1-diarylmethane structures were constructed in good yields with complete regioselectivity. Finally, the researchers succeeded in the late-stage functionalization of some biologically aromatic molecules using only a fluorinating agent such as selectfluor or HF as a stoichiometric oxidant.

In 2022, Wang and co-workers utilized Na₂-eosin Y for the photocatalytic difluoroalkylation of benzylic C(sp³)–H bond **92**

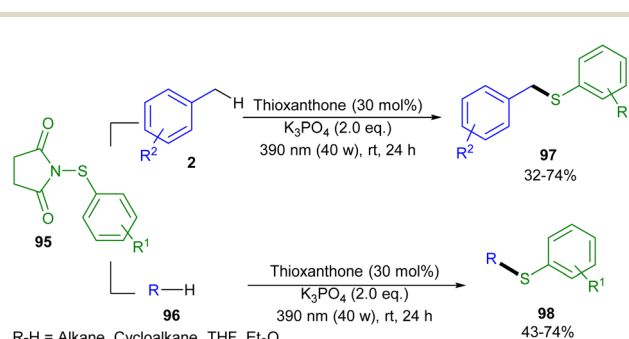


Scheme 59 Benzylic C(sp³)–H difluoroalkylation with difluoroenoxy silanes via photoredox catalysis (Wang and co-workers).⁵⁶

by using difluoroenoxy silanes **93** (Scheme 59).⁵⁶ In general, the reaction proceeded through the formation of benzyl radical **A** through a HAT process using singlet O₂. Then, the conversion of **A** into carbocation **B** occurred in the presence of 'OOH. After that, the nucleophilic addition of difluoroenoxy silane **93** to the carbocation led to the final product **94**. Xanthenes, acridines and thioxanthene reacted well with difluoroalkylating reagents, yielding 38–96% of products. The method featured the use of an organic photocatalyst, a green oxidant of air and mild conditions. The evaluation results indicated that transition metal catalysts Ru(bpy)₃Cl₂ and [Ir(dtbbpy)(ppy)₂]PF₆ suppressed the reaction, while organocatalysts Mes-Acr⁺ClO₄⁻, Rose Bengal, 9-fluorenone and 9,10-dicyanoanthracene gave moderate chemical yields. Further synthetic transformations of the products including the conversion of the ketone moiety into the alcohol, and the removal of the benzoyl group to access the CF₂H group were also performed in this work.

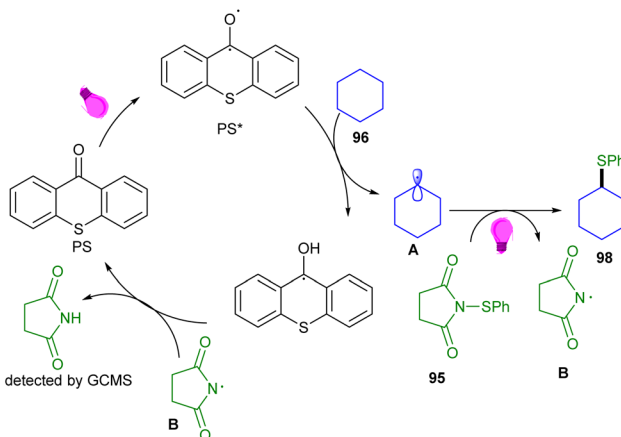
In 2023, Maiti and co-workers established C(sp³)–H thioarylation of toluene derivatives using thioxanthone as a photocatalyst (Scheme 60).⁵⁷ Thioxanthone played a dual role in the hydrogen atom transfer and energy transfer. First, under 390 nm light, thioxanthone (PS) was excited to triplet PS*, which abstracted a hydrogen atom from the C(sp³)–H bond of **96**. Two thioaryl and succinyl radicals were generated *via* energy transfer from thioxanthone. In the next step, a thioaryl radical was coupled with a benzylic radical to provide the coupling product **98** (Scheme 61). However, a succinyl radical regenerated thioxanthone to restart the catalytic cycle. The post-functionalization of the thioarylated product with a bromo group was investigated for the Suzuki–Miyaura and Sonogashira cross-coupling reactions. Besides, these sulfide products could be oxidized to sulfoxides or converted to the corresponding disulfides.

In 2022, the Das research team developed a new and simple strategy for the upcycling of polystyrene-based wastes into lower weight aromatics, namely benzoic acids, aromatic ketones, benzene and toluene (Scheme 62).⁵⁸ The reaction was performed in the absence of any transition metals under mild conditions. The protocol was demonstrated on 13 varieties of real-life plastics on the gram scale, and showed good synthetic utility in the synthesis of bioactive compounds. In general, under LED irradiation, three HAT cycles including NBS,

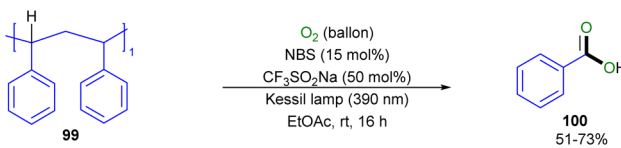


Scheme 60 Photo-induced HAT-assisted C(sp³)–H thioarylation (Maiti and co-workers).⁵⁷



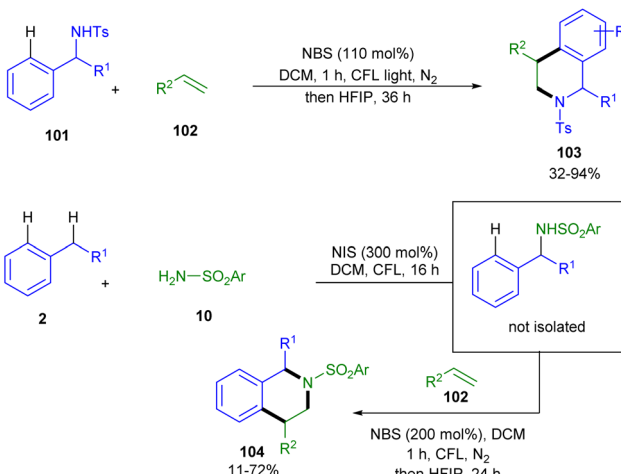


Scheme 61 Plausible mechanism for photo-induced HAT-assisted $C(sp^3)$ -H thioarylation.

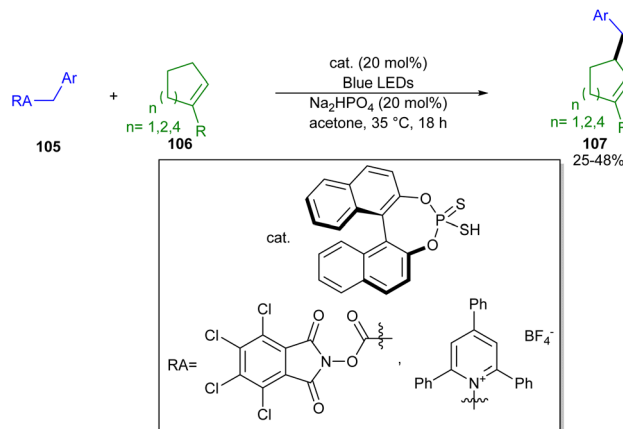


Scheme 62 Upcycling of polystyrene-based wastes into low weight aromatics (Das and co-workers).⁵⁸

CF_3SO_2Na and O_2 can afford the radicals that abstract a hydrogen radical from polystyrene, generating the benzylic radical, which under the attack of O_2 and subsequent β -scission produced smaller fragments. In 2024, a photo-induced reaction involving toluene derivatives **2**, **101**, sulfonamides **10** and olefins **102** was reported by Li's research team (Scheme 63).⁵⁹ A series of tetrahydroisoquinolines **104** were isolated through a one-pot two-step process. First, the amination of benzylic $C(sp^3)$ -H bonds by sulfonamides in the presence of NBS as an oxidant and a compact fluorescent lamp (CFL) was performed.



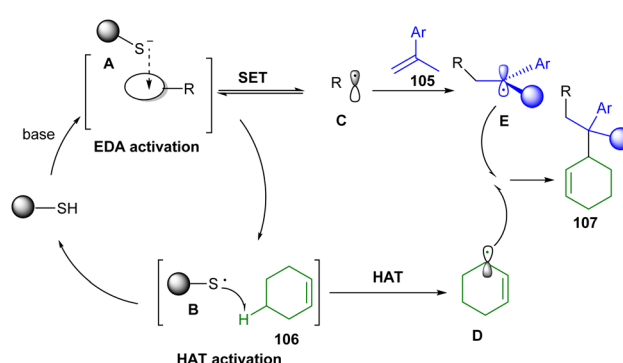
Scheme 63 Reaction of toluene derivatives with sulfonamides and olefins (Li and co-workers).⁵⁹



Scheme 64 Photoredox catalytic allylation of benzylic $C(sp^3)$ -H bonds (Melchiorre and co-workers).⁶⁰

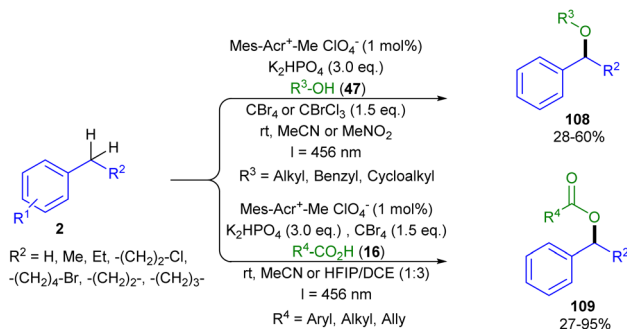
Then, the olefin coupling was carried out through (2 + 4) cycloaddition *via* a radical bond formation and a polar bond formation. This feature of this synthetic method allows the incorporation of various bifunctional reagents in the synthesis of N-heterocycles. The method was also investigated using benzylsulfonamide and olefin under the same conditions.

In 2022, Melchiorre and co-workers used a photoredox catalyst to perform the coupling of $C(sp^3)$ -H bonds of toluene derivatives with $C(sp^3)$ -H bonds of nonfunctionalized allylic substrates (Scheme 64).⁶⁰ In this process, benzylic and allylic radicals were generated under visible light irradiation with the assistance of photoredox catalysts. A dithiophosphoric acid was used as a catalyst playing two roles, the first as a catalytic donor to create photoactive electron donor-acceptor (EDA) complexes and the second as a hydrogen atom abstractor. To show the precise mechanism, the authors designed a three-component route for the coupling reaction driven by visible light. They compensated less reactivity of non-stabilized alkyl radicals by intercepting nonstabilized alkyl radicals **C**, generated upon catalytic EDA activation of a radical precursor, with styrene **106** to form stable benzylic radical **E**. However, radical **D** was generated through a HAT process between a thiy radical **B** and an allylic precursor. Finally, the benzylic radical **VI** coupled with radical **D** to yield the final product **107** (Scheme 65).



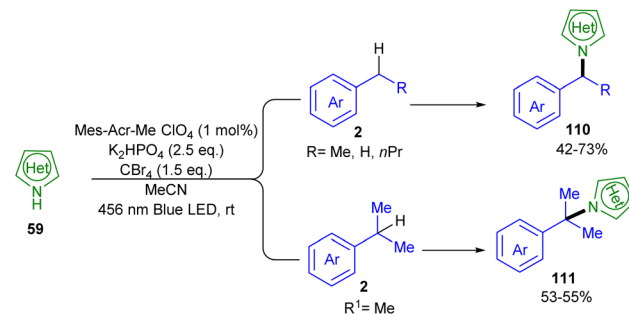
Scheme 65 Rational mechanism for photoredox catalytic allylation of benzylic $C(sp^3)$ -H bonds.





Scheme 66 Benzyllic $C(sp^3)$ -H etherification and esterification reactions via photoredox catalysis (Das and co-workers).⁶¹

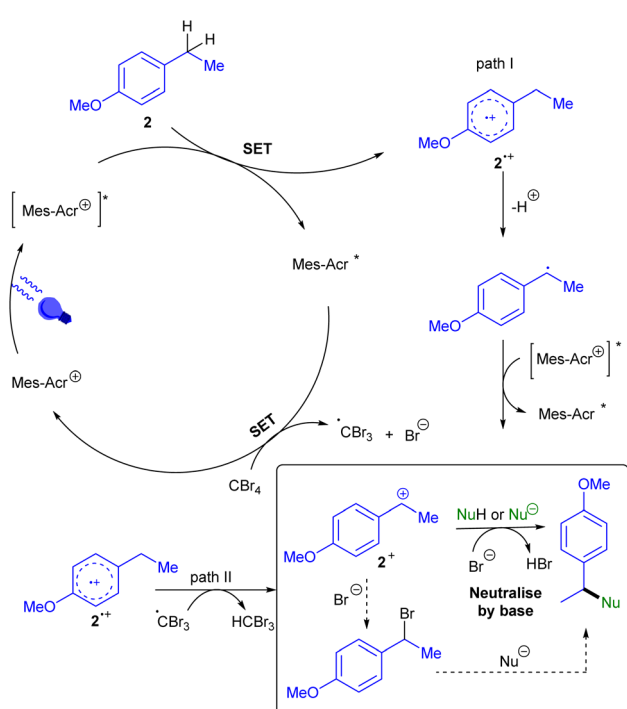
In 2022, the Das group established etherification and esterification reactions of benzylic $C(sp^3)$ -H bonds by using a photoredox catalyst under mild conditions (Scheme 66).⁶¹ In this regard, a diverse range of aliphatic alcohols and aliphatic/aromatic carboxylic acids as well as amino acids acted as nucleophiles in the reaction with toluene derivatives, leading to regioselective synthesis of benzylic ether and ester products. Additionally, late-stage functionalization etherification and esterification of 20 pharmaceutically relevant molecules was carried out in this work. It was found that the reaction started with the formation of an excited state of the photocatalyst and oxidized 2 through the SET process to form a radical cation 2^+ . The reaction of this cation radical with the base generated a benzyl radical. However, CBr_4 via the SET process afforded a tribromomethyl radical. Two possible pathways could be



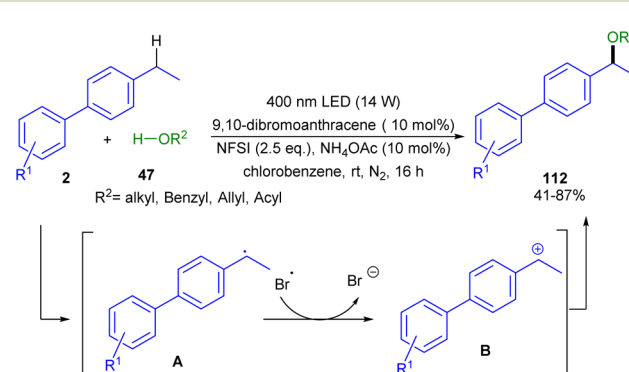
Scheme 68 Benzyllic $C(sp^3)$ -H amination reactions via photoredox catalysis (Das and co-workers).⁶²

attributed in this step. Pathway I carried out by further oxidation of 2^+ to carbocation 2^+ . In path II, the tribromomethyl radical as a HAT reagent abstracted a hydrogen atom from 2^+ to obtain carbocation 2^+ , followed by reaction with nucleophiles to furnish the final product (Scheme 67). After a year, the same group reported benzylic $C(sp^3)$ -H bond amination using this photoredox catalyst (Scheme 68).⁶² In this regard, a diverse range of heterocyclic amines (pyrazole, indazole, triazole, etc.) were utilized as nucleophiles, leading to benzylic amine frameworks 110–111. 9-Mesityl-10-methylacridinium perchlorate ($Mes-Acr^+-Me ClO_4^-$) as a photocatalyst promoted the formation of both the benzylic radicals and the tribromomethyl radical CBr_3 from alkylarene and CBr_4 , respectively, through the SET process. After that, the radical CBr_3 abstracted a hydrogen atom from benzylic radical to generate $CHBr_3$ and benzylic carbocation. The benzylic carbocation then reacted with the aminating agent to construct the target product.

Visible light-induced alkoxylation of benzylic C-H bond of alkyl biphenyls 2 with alcohols 47 was reported by Dai and Liu in 2023 (Scheme 69).⁶³ In this work, 9,10-dibromoanthracene acted as a photocatalyst and *N*-fluorobenzenesulfonimide served as an oxidant. Alkyl biphenyls with electron-donating groups (such as methoxy and *tert*-butyl) displayed a higher reactivity than that of electron-attracting groups. However, the position and number of substituents on the phenyl ring had little influence on the substrate reactivity, while changing the



Scheme 67 Plausible mechanism for benzyllic $C(sp^3)$ -H etherification and esterification reactions via photoredox catalysis.



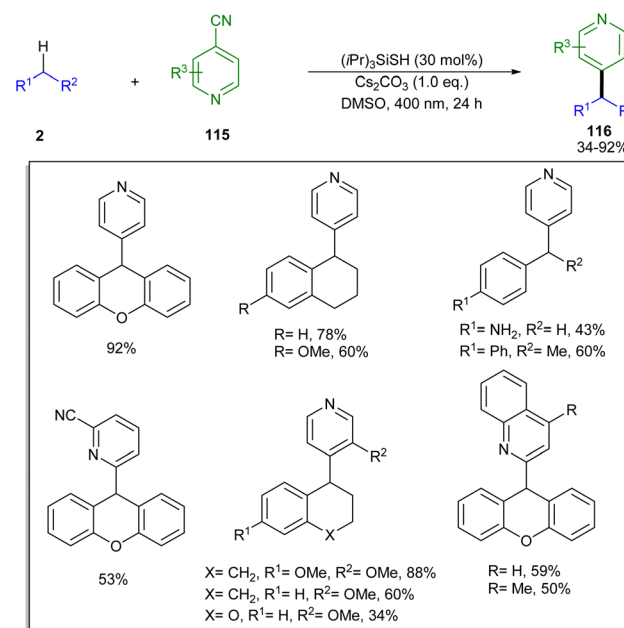
Scheme 69 Visible light-driven organocatalytic alkoxylation of benzyllic C-H bonds (Dai and co-workers).⁶³



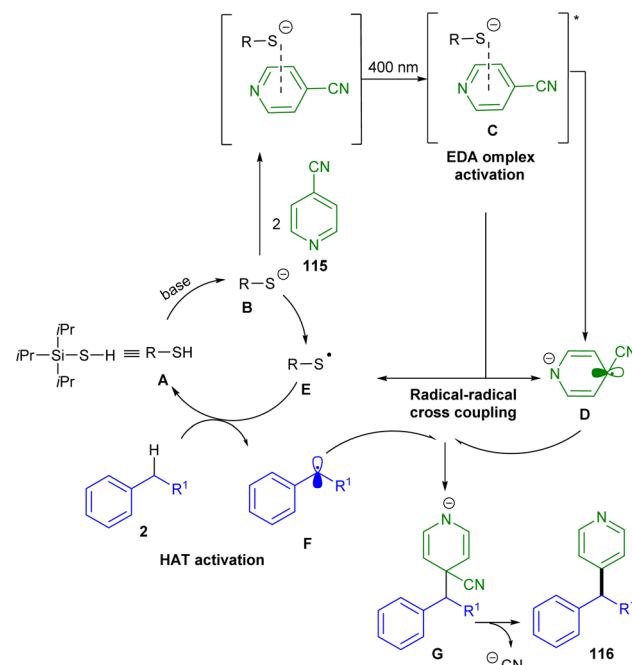
position of the phenyl group from the *para* of alkylbenzene to the *ortho* or *meta* resulted in a decrease in reactivity. A radical reaction pathway was proposed for this reaction, involving a HAT process for the formation of radical **A** from alkyl biphenyl **2**, followed by a SET process to form benzyl cation intermediate **B**. The final benzyl ether product **112** was furnished *via* the attack of alcohol on the carbocation **B**.

Developing a transition metal- and photocatalyst-free visible light-induced synthetic method for the functionalization of the benzylic $C(sp^3)$ -H bond with fluorenones was reported by the Chen team (Scheme 70).⁶⁴ Electron-donating groups in toluene derivatives exhibited better reactivity than electron-deficient ones. However, the electronic effect was opposite in the case of fluorenones as coupling partners. The procedure involved the ketyl radicals **C** and benzyl radicals **B** generated through the conversion of fluorenone **113** to diradical **A**, followed by the HAT process at the benzylic C-H site of **2**. Afterward, the cross-coupling of reactive radical **B** and stable radical **C** gave rise to the desired fluorenol. The gram-scale synthesis of product (1.18 g, 78% yield) and further dehydration, deoxygenation, azidation, and Friedel-Crafts alkylation of the fluorenol products were also performed in this work.

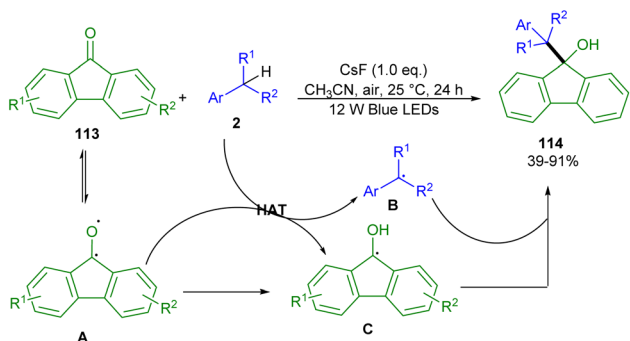
A transition metal- and photocatalyst-free strategy was suggested for the heteroarylation of the benzylic $C(sp^3)$ -H bonds (Scheme 71).⁶⁵ In this regard, a diverse range of alkylarenes were treated with 4-cyanopyridines in the presence of triisopropylsilanolthiol (iPr_3SiSH) as an organocatalyst. Therefore, iPr_3SiSH not only helped in generating an electron donor-acceptor complex (EDA) but also acted as a hydrogen atom transfer catalyst, towards alkyl/benzylic radicals from the $C(sp^3)$ -H bonds. Several mechanistic investigations such as radical scavenging experiments, and light on/off experiments revealed the involvement of a radical route and the necessity of a light source for the reaction to proceed. Based on these results, a plausible mechanism was proposed, which involved the initial deprotonation of HAT source **A** (iPr_3SiSH) by Cs_2CO_3 to obtain electron-rich thiolate anion **B**. The reaction of **B** with 4-cyanopyridine **115** gave rise to a photoactive EDA complex **C** upon light excitation. After that, a light-induced SET process occurred in **C** to afford a pyridine radical anion **D** and a thiol radical **E**. The latter abstracted a hydrogen atom (H^+) from the $C(sp^3)$ -H bond of **2**, to render a benzylic radical **F**, which coupled with



Scheme 71 Visible light-induced redox-neutral heteroarylation of $C(sp^3)$ -H bonds (Rueping and co-workers).⁶⁵



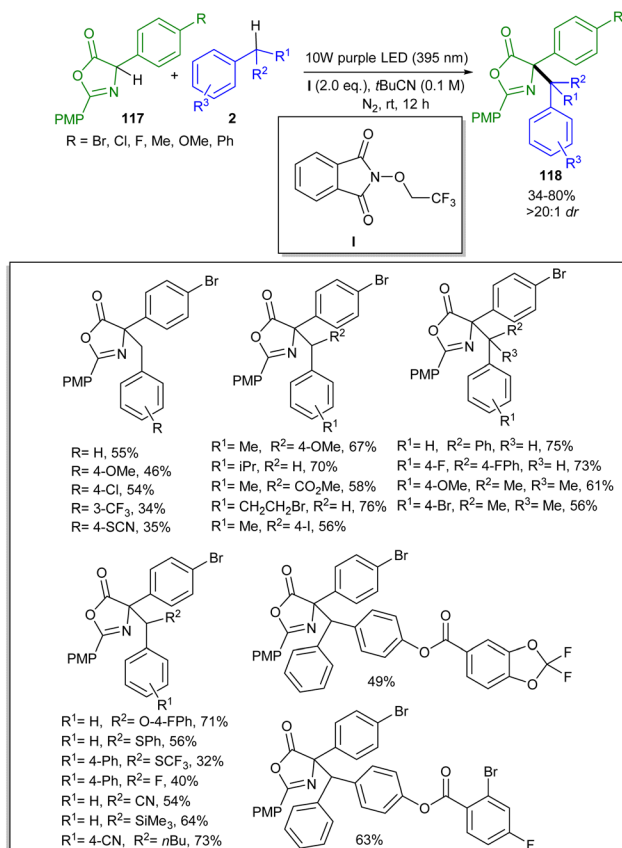
Scheme 72 Reasonable mechanism for visible light-induced redox-neutral heteroarylation of $C(sp^3)$ -H bonds.



Scheme 70 Benzylic C-H functionalization with fluorenones under visible light irradiation (Chen and co-workers).⁶⁴

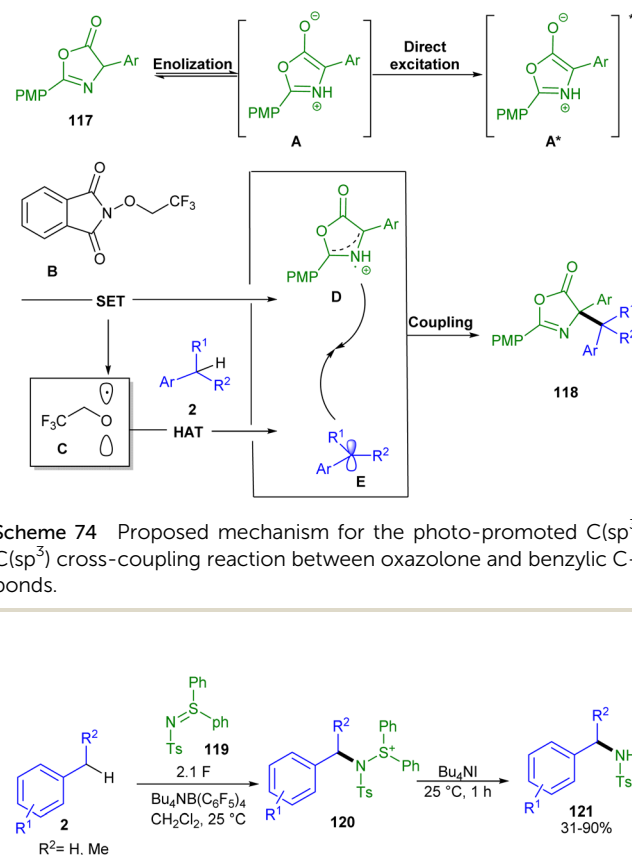
radical **D** to yield intermediate **G**. Ultimately, **G** lost a CN anion to deliver product **116** (Scheme 72). Furthermore, the synthetic utility of this method was showed by the gram-scale synthesis of product (1 g, 72%), and also the introduction of the pyridine into a drug molecule *via* late-stage modification (an antihistaminic analogue, 46%).



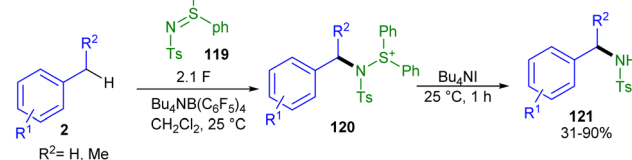


Scheme 73 Photo-promoted $\text{C}(\text{sp}^3)\text{-C}(\text{sp}^3)$ cross-coupling reaction between oxazolone and benzylic C-H bonds (Zheng and co-workers).⁶⁶

The synthesis of amino acid derivatives **118** can be obtained through the $\text{C}(\text{sp}^3)\text{-C}(\text{sp}^3)$ cross-coupling reaction between oxazolone **117** and a wide variety of benzylic C-H bonds **2** (Scheme 73).⁶⁶ Primary, secondary, tertiary, diarylmethanes, and functionalized structures such as benzyl fluoride, benzyl chloride, benzyl cyanide, benzyl(trifluoromethyl)sulfane, and benzyltrimethylsilane as well as complex structures can successfully participate in this coupling reaction, offering direct metal-free route access to sterically hindered α,β -tetrasubstituted α -tertiary amino acids. Avoiding transition metal catalysts, photocatalysts, or redox agents, and performing the reaction at room temperature make this method sustainable and environmentally friendly. Various mechanistic studies including KIE, radical trapping, and cyclic voltammetry experiments revealed the plausible mechanism, starting with the irradiation of light to obtain the excited state **A*** from oxazolone enolate **A**. The SET reaction in bench-stable *N*-alkoxyphthalimide **B** generated the highly electrophilic trifluoroethoxy radical **C** and oxazolone radical **D**. The trifluoroethoxy radical **C**, the key intermediate, acted as a HAT reagent, abstracting a hydrogen atom from alkane **2** to produce alkyl radical **E**. In the next step, **E** coupled with **D** to furnish product **118** (Scheme 74).



Scheme 74 Proposed mechanism for the photo-promoted $\text{C}(\text{sp}^3)\text{-C}(\text{sp}^3)$ cross-coupling reaction between oxazolone and benzylic C-H bonds.

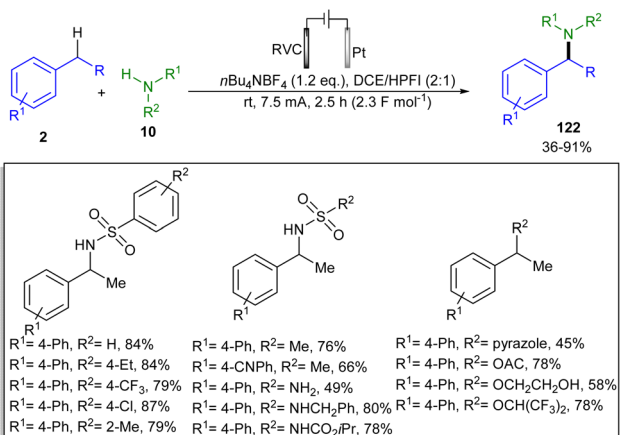


Scheme 75 Electrochemical C-H amination of toluene derivatives (Yoshida and co-workers).⁶⁷

2.6. $\text{C}(\text{sp}^3)\text{-H}$ functionalization using electrochemical method

In 2017, electrochemical benzylic $\text{C}(\text{sp}^3)\text{-H}$ amination was performed by Yoshida and colleagues (Scheme 75).⁶⁷ The method presented two-step one-pot electrochemical oxidation of toluene derivatives **2** by *N*-tosyldiphenylsulfilimine reagent **119** into benzylaminosulfonium ions **120**. The high oxidation potential and nucleophilicity of *N*-tosylsulfilimine made it an active reagent in the coupling reaction with a wide range of xylenes, toluene and toluene derivatives bearing electron-donating, electron-withdrawing and halogen groups. In the next step, a series of *N*-tosylbenzylamines **121** were obtained through nucleophilic attack of Bu_4NI to benzylaminosulfonium ions under non-electrolytic conditions. In addition to *N*-tosylsulfilimine, sulfilimine with a benzoyl (Bz) group also showed good nucleophilicity, but sulfilimine with the 4-nitrobenzenesulfonyl (Nos) group did not work owing to its low nucleophilicity. Another electrochemical $\text{C}(\text{sp}^3)\text{-H}$ amination of toluene derivatives **2** with sulfonamides **10** was reported by Xu and his colleagues in 2020 (Scheme 76).⁶⁸ The process involved anodic cleavage of benzylic $\text{C}(\text{sp}^3)\text{-H}$ to obtain a carbocation intermediate, which was then trapped by an amine nucleophile. HFIP as the co-solvent can modulate the oxidation ability of both toluene **2** and the aminated product **122** to avoid over-oxidation of the latter. Other nucleophilic reactants such as

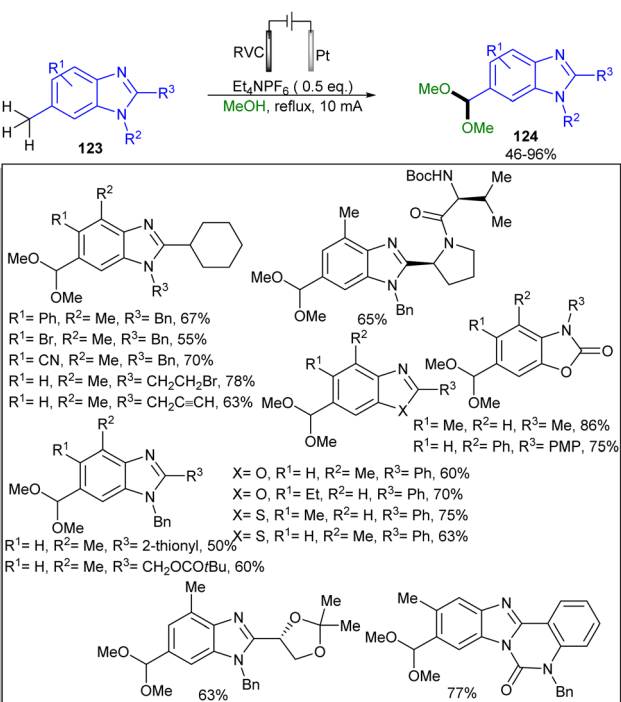




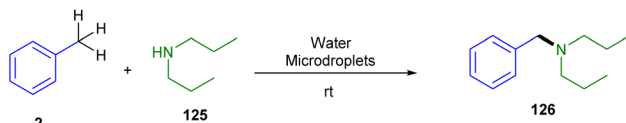
Scheme 76 Electrochemical C–H amination of toluene with amine and oxygen nucleophiles (Xu and co-workers).⁶⁸

pyrazole, acetate, ethylene glycol, and HFIP were also compatible, leading to the formation of corresponding products in good yields.

Using the electrochemical method, highly site-selective benzylic electrooxidation of methylarenes can be performed in the absence of any transition metal catalysts or chemical oxidants (Scheme 77).⁶⁹ Et_4NPF_6 as the electrolyte and MeOH as both the reactant and solvent resulted in the conversion of a diverse range of methyl benzoheterocycles **123** to the corresponding aromatic acetals **124**. These aromatic acetals can be easily converted to aromatic aldehydes *via* hydrolysis in one-pot or in a separate step. The mechanistic investigations and DFT



Scheme 77 Site-selective electrooxidation of methylarenes with MeOH (Cheng and co-workers).⁶⁹

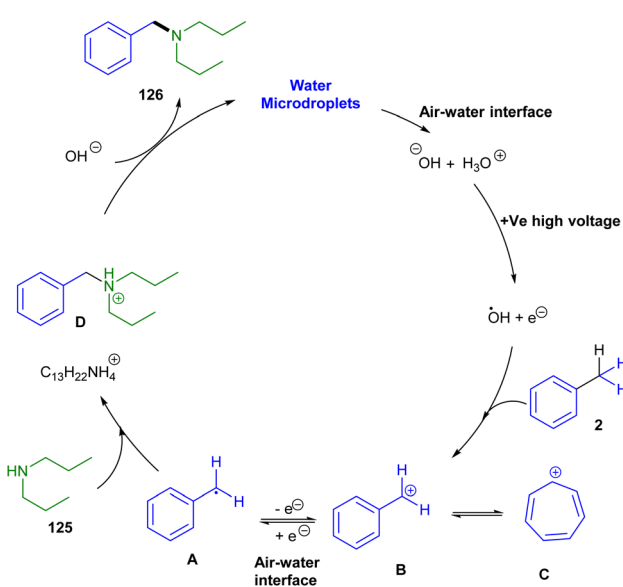


Scheme 78 $\text{C}(\text{sp}^3)\text{-H}$ amination of toluene with amine in the presence of water microdroplets (Gnanamani and co-workers).⁷⁰

calculations suggested that the reaction may proceed *via* a single electron transfer oxidation reaction of the benzene nucleus to a radical cation, followed by methylation of the benzylic $\text{C}(\text{sp}^3)\text{-H}$ bonds. This method was also applicable to the synthesis of the antihypertensive drug telmisartan.

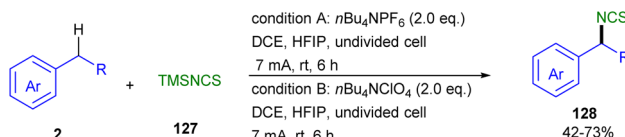
Water microdroplets can show a unique reactivity over bulk water or other solvents (Scheme 78).⁷⁰ Water microdroplets can be decomposed into H_3O^+ cations and OH^- anions, which resulted in OH radicals in the presence of high voltage. In water microdroplets, stable C_7H_7^+ cations **D** were generated from toluene and H_3O^+ cations in the presence of a positive voltage (+4 kV). Both C_7H_7^+ cations and $\text{C}_6\text{H}_5\text{CH}_2^\cdot$ radicals **B** were generated *via* hydroxyl radicals at the water–gas interface of microdroplets. A wide range of dissolved primary, secondary, and tertiary amines in microdroplets can easily react with C_7H_7^+ and $\text{C}_6\text{H}_5\text{CH}_2^\cdot$ species to generate the protonated amine **F** *via* $\text{C}(\text{sp}^3)\text{-N}$ bond formation. The removal of a proton from **F** by a hydroxyl anion led to benzylamine **126** (Scheme 79). The scope of the substrates could be expanded to other electrophiles and nucleophiles.

Electrochemical isothiocyanation of toluene derivatives **2** with TMSNCS **127** was reported by Guo and co-workers in 2022 (Scheme 80).⁷¹ The procedure has the advantages of high regio- and chemoselectivity, and the performance of the reaction in the absence of external oxidants under mild conditions. The high chemoselectivity is due to the *in situ* isomerization of

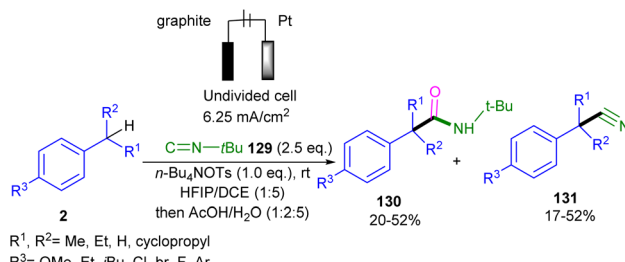


Scheme 79 Rational mechanism for the $\text{C}(\text{sp}^3)\text{-H}$ amination of toluene with amine in the presence of water microdroplets.





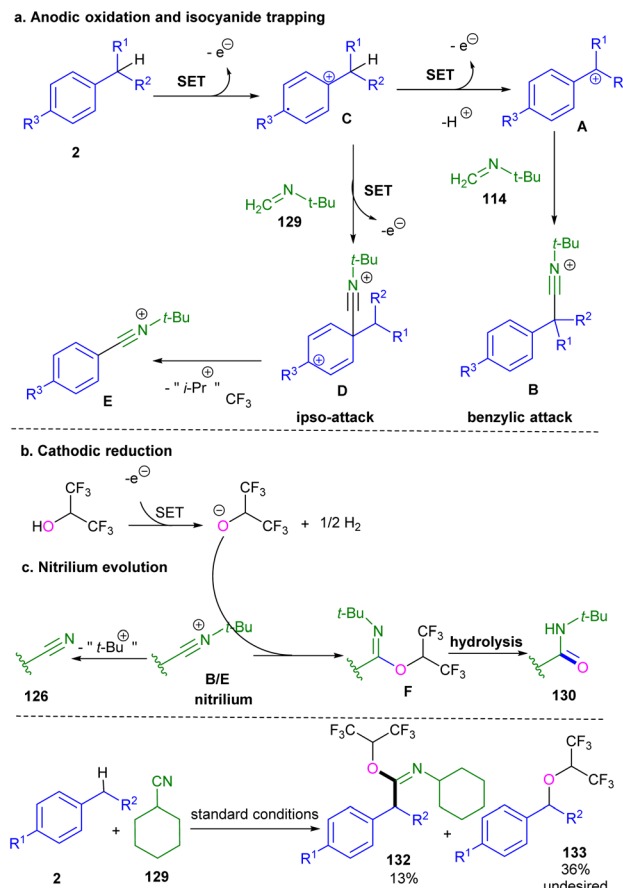
Scheme 80 Electrochemical $C(sp^3)$ -H isothiocyanation of toluene with TMSNCS (Guo and co-workers).⁷¹



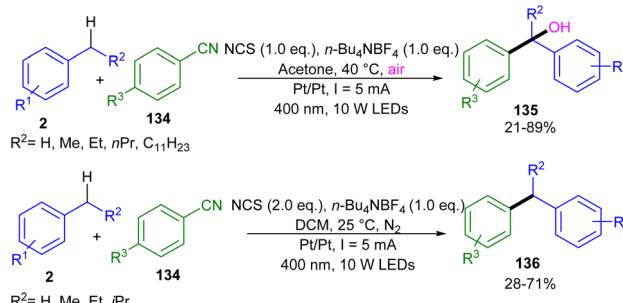
Scheme 81 Electrochemical carbamoylation and cyanation of benzylic $C(sp^3)$ -H bonds (Vincent and co-workers).⁷²

benzylic thiocyanates to isothiocyanates. The applicability of this method was demonstrated by the isothiocyanation of various pharmaceuticals and complex molecules under these conditions and also the synthesis of bioactive thioureas *via* one-pot two-step $C(sp^3)$ -H isothiocyanation of tetrahydronaphthalene or 4-fluoroethylbenzene. Another report on the electrochemical C-H activation functionalization of toluene derivatives was described by Vincent and his team (Scheme 81).⁷² In this method, they performed carbamoylation and cyanation of benzylic $C(sp^3)$ -H bonds with an isocyanide reagent. According to the reaction mechanism in Scheme 82, direct anodic oxidation of the phenyl ring of **2** generated radical cation **C**. Depending on the substitution pattern of the arene, intermediate **C** was proceeded through two different pathways. The substituent at the para site made intermediate **C** lose a proton towards the benzyl radical, which was oxidized to the benzylic carbocation **A**, followed by the interaction with *t*-BuNC to yield nitrilium **B**. This intermediate can either be converted into the cyano derivative **131** *via* losing a *tert*-butyl cation or generate imide **F** by capturing the alkoxide of HFIP and hydrolyze to amide **130**. In the presence of an isopropyl group, ipso attack of **129** to intermediate **C** led to intermediate **D**, which underwent aromatization to give a relatively stable isopropyl secondary carbocation **E**. This intermediate can also react with HFIP to generate intermediate **F**, which then furnished benzamide **130** after hydrolysis. However, for less nucleophilic isocyanide like cyclohexyl isocyanide, the benzylic cation could competitively be trapped by HFIP to yield **133**.

In 2023, Wang and co-workers introduced a switchable methodology for the arylation of $C(sp^3)$ -H bonds (Scheme 83).⁷³ Two different products of diaryl alcohols **135** and diaryl alkanes **136** were synthesized by changing the reaction solvent. Both products were obtained in the large-scale experiment: 1.14 g, 85% yield for the aryloxygenation product and 1.01 g, 70% yield for the arylation product. In the case of arylation product, in the



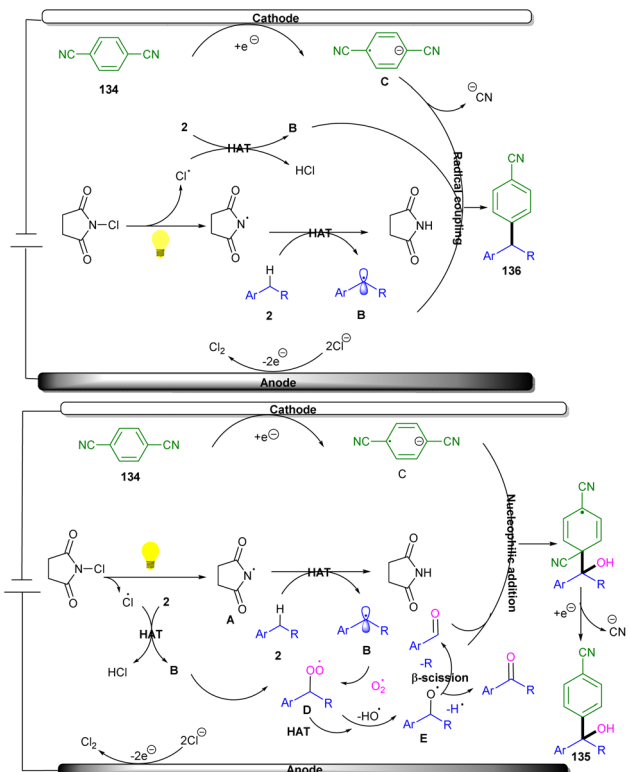
Scheme 82 Possible mechanism for the electrochemical carbamoylation and cyanation of benzylic $C(sp^3)$ -H bonds.



Scheme 83 Electrochemical oxygenative arylation of $C(sp^3)$ -H bonds (Wang and co-workers).⁷³

presence of visible light irradiation, the N-Cl bond of NCS was cleaved to obtain a chlorine radical and succinimide radical **A**. Benzyl radical **B** was obtained from the abstraction of a hydrogen from alkylbenzene **2** by the succinimide radical **A** or by a hydrogen transfer process by the chlorine radical. Then, the benzyl radical **B** coupled with the anion radical **C** to form product **135** along with the elimination of a cyanide anion. In the presence of an oxygen source, benzyl radical **B** abstracted an oxygen atom to form superoxide radical **D**, followed by hydrogen atom transfer and the homolysis to render an alkoxy

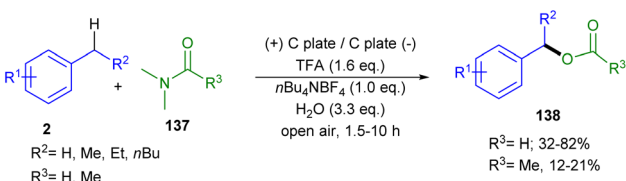




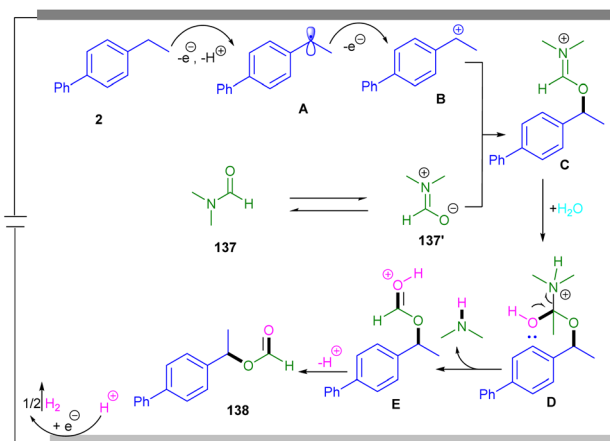
Scheme 84 Two plausible pathways for electrochemical arylation of $C(sp^3)$ -H bonds.

radical E. The β -scission of E afforded aldehyde and an alkyl radical. The nucleophilic anion radical C attacked ketone or aldehyde to obtain intermediate F, which was reduced to product 135 or 136 by the cyanide elimination similar to the arylation process (Scheme 84).

Electrochemical formyloxylation of benzylic $C(sp^3)$ -H bonds with DMF can be efficiently performed without the need for transition metals or oxidants (Scheme 85).⁷⁴ A broad spectrum of alkyl phenyls bearing OMe, Ph and OPh groups as well as alkyl diphenyls bearing halogens such as F, Cl, Br, and I, and electron-withdrawing groups such as CN, CF₃, CHO, COMe, CO₂H, and CO₂Et were compatible in this reaction. Generally, acetamides showed higher product yields than those of formamides, confirming the higher reactivity of the acyl moiety in the acetamides. As illustrated in Scheme 86, toluene 2 was converted into the benzylic radical B under electrochemical conditions. The further oxidation of B led to the carbocation C,



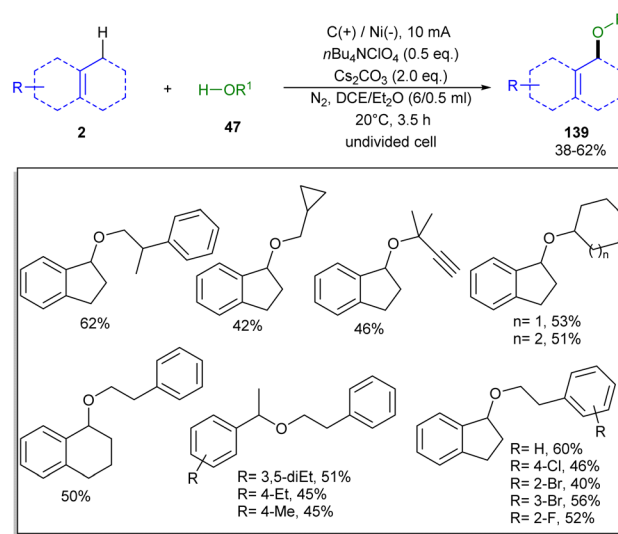
Scheme 85 Electrochemical formyloxylation of benzylic $C(sp^3)$ -H bonds with DMF (Guan and co-workers).⁷⁴



Scheme 86 Possible mechanism for the electrochemical formyloxylation of benzylic $C(sp^3)$ -H bonds with DMF.

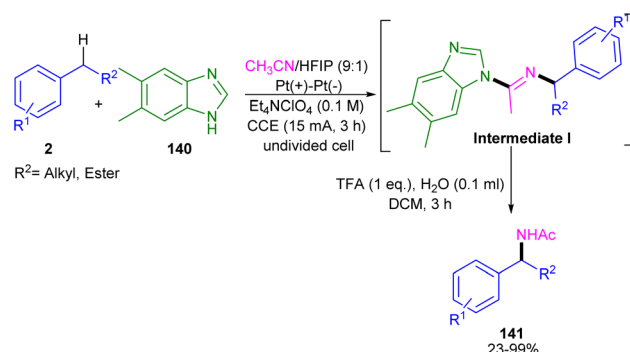
which under nucleophilic attack of anion A gave an iminium intermediate D. The hydrolysis of D in aqueous media afforded the desired product 135 along with the generation of amine and H_2 molecules. Another study on the electrochemical oxygenation of the benzylic C-H bonds 2 with aliphatic alcohols 47 was reported by Wang and co-workers (Scheme 87).⁷⁵ By applying various aliphatic alcohols, benzylic and allylic compounds as feedstock, etherification occurred with high efficiency, leading to the formation of desired product 139 in acceptable yields.

In 2023, the benzylic C(sp^3)-H amination was performed as a three-component reaction between toluene derivatives 2, benzimidazole 140 and acetonitrile (Scheme 88).⁷⁶ In this protocol, benzimidazoles acted as reactive N-radicals that were able to participate in the electrochemical benzylic C-H amination as selective HAT mediators. With these N-radicals, novel site-selectivity and reactivity were observed, which was applicable for the amination of not only benzylic C(sp^3)-H but also



Scheme 87 Electrochemical etherification of benzylic C-H bonds with alcohols (Wang and co-workers).⁷⁵

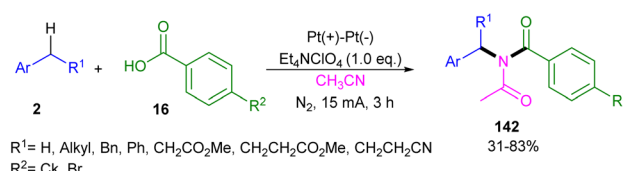




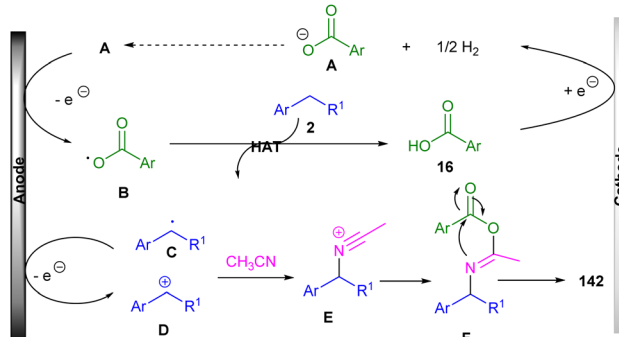
Scheme 88 Benzyl C(sp^3)-H amination in the presence of benzimidazole and acetonitrile (Zhang and co-workers).⁷⁶

allylic C(sp^3)-H and β -C(sp^3)-H of alcohols. The N-radical intermediate was confirmed by EPR, UV-vis spectroscopy, and HRMS analysis. The KIE experiment (2.85/1) suggested that the formation of the benzylic radical occurs in the rate-determining step. According to the control experiment, a plausible mechanism was proposed that started with the oxidation of benzimidazole **140** to N-radical **A** through a proton-coupled electron transfer (PCET) process with the assistance of alkoxide anion **E** generated in the cathode. Subsequently, radical **A** trapped a hydrogen atom from toluene **2** to form the benzylic radical **B**, which then underwent SET to yield carbocation **C**. Upon a classic Ritter process by incorporation with acetonitrile, carbocation **C** was converted into nitrilium **D**. Then, the nucleophilic attack of benzimidazole to nitrilium **D** provided intermediate **I**. The final aminated product **141** was obtained after a hydrolysis step under acidic conditions (Scheme 89).

In 2024, Qian *et al.* developed an electrochemical approach for the three-component reaction between benzylic C(sp^3)-H bonds **2**, benzoic acids **16** and CH_3CN (Scheme 90).⁷⁷ The reaction route was confirmed by several mechanistic studies,



Scheme 90 Electrochemical benzylic C(sp^3)-H amidation using benzoic acid and acetonitrile (Qian and co-workers).⁷⁷



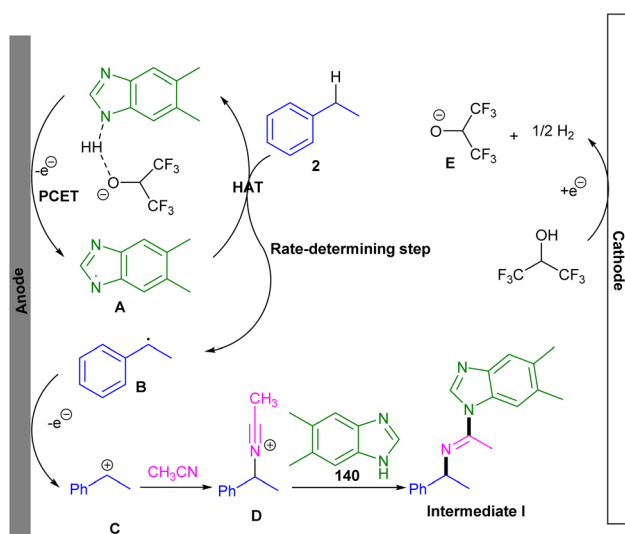
Scheme 91 Rational mechanism for electrochemical benzylic C(sp^3)-H amidation using benzoic acid and acetonitrile.

including the kinetic isotope effect, radical scavenger experiment, and cyclic voltammograms. The results of KIE ($K_{\text{H}}/K_{\text{D}} = 2.2/1$) indicated that the benzylic C(sp^3)-H activation is a rate-determining step and radical scavenger experiments suggested the involvement of a radical pathway in this reaction. The method was based on the *in situ*-generated oxygen-centered radicals **A** from benzoic acids in the anode side, which under a HAT process caused the conversion of toluene derivatives into the benzylic radical. Again, in the anode, the benzylic radical **C** could be converted into the benzylic cation **D**, which underwent the nucleophilic attack of CH_3CN , affording the cation **E**. This cation was subjected to the oxygen attack of benzoate to furnish product **142**. It should be noted that in the cathodic surface, benzoic acid could be reduced into benzoate **A** (Scheme 91).

3. Conclusions

In this review, we described the direct activation/functionalization reactions of benzylic C(sp^3)-H bonds. The transformations were accomplished in the absence of transition metal catalysts.

In most cases, oxidants were used, which generated free radicals, driving the reactions through a free radical mechanism. Two radical scavengers, namely TEMPO and BHT, were frequently used in most of these reactions to study the radical pathway. The dramatic decrease in the product yield indicates the key role of the oxidant in progression of the radical reaction. Organophotocatalysts or non-metal catalysts were used in these reactions, or the reactions were carried out without any catalyst, offering environmentally friendly, cost-effective, and atom-economic C–H benzylic functionalization reactions. However,



Scheme 89 Plausible mechanism for benzyl C(sp^3)-H amination in the presence of benzimidazole and acetonitrile.



these metal-free transformations still have some limitations such as the use of stoichiometric amounts of chemical oxidants and bases, which leads to negative environmental impacts. Another obstacle is the poor selectivity in these types of C–H activation reactions, which must be controlled by the careful selection of the non-metal catalysts, ligands, additives or steric effects. In addition, more efforts should be made to identify the exact reaction mechanism and the role of non-metal catalysts and additives.

Furthermore, the synthesis of drugs and drug intermediates under metal-free conditions will be a challenge for researchers. The development of new powerful methods by adopting low-cost, eco-friendly, and non-metal catalysis systems is important for the extensive application of direct C(sp³)–H functionalization strategies. Therefore, progress in transition metal-free C(sp³)–H activation/functionalization reactions could open a promising avenue for the synthesis of biologically important molecules. As mentioned in this context, several research groups have recently tried to use simple and sustainable methods such as photochemistry and electrochemistry for benzylic C(sp³)–H activation. These methods appear to be alternative routes to hazardous transition metal catalysts and chemical oxidants in the near future. We believe that this review will inspire organic chemists to engage more in this area of chemistry.

Data availability

Data sharing is not applicable to this review article as no new data were created or analyzed in this study.

Conflicts of interest

There are no conflicts to declare.

Notes and references

- 1 C.-L. Sun and Z.-J. Shi, *Chem. Rev.*, 2014, **114**, 9219–9280.
- 2 A. Batra and K. N. Singh, *Eur. J. Org. Chem.*, 2020, **2020**, 6676–6703.
- 3 V. P. Mehta and B. Punji, *RSC Adv.*, 2013, **3**, 11957–11986.
- 4 T. L. Chan, Y. Wu, P. Y. Choy and F. Y. Kwong, *Chem.–Eur. J.*, 2013, **19**, 15802–15814.
- 5 J.-R. Chen, X.-Q. Hu, L.-Q. Lu and W.-J. Xiao, *Chem. Soc. Rev.*, 2016, **45**, 2044–2056.
- 6 H. Yi, G. Zhang, H. Wang, Z. Huang, J. Wang, A. K. Singh and A. Lei, *Chem. Rev.*, 2017, **117**, 9016–9085.
- 7 S. Mandal, T. Bera, G. Dubey, J. Saha and J. K. Laha, *ACS Catal.*, 2018, **8**, 5085–5144.
- 8 J.-L. Tu, Y. Zhu, P. Li and B. Huang, *Org. Chem. Front.*, 2024, **11**, 5278–5305.
- 9 M. Oliva, G. A. Coppola, E. V. Van der Eycken and U. K. Sharma, *Adv. Synth. Catal.*, 2021, **363**, 1810–1834.
- 10 C. Chenyi and Z. Dong, *Chin. J. Org. Chem.*, 2022, **42**, 1586.
- 11 R. Yazaki and T. Ohshima, *Tetrahedron Lett.*, 2019, **60**, 151225.
- 12 B. Liégault, J.-L. Renaud and C. Bruneau, *Chem. Soc. Rev.*, 2008, **37**, 290–299.
- 13 I. Bosque, R. Chinchilla, J. C. Gonzalez-Gomez, D. Guijarro and F. Alonso, *Org. Chem. Front.*, 2020, **7**, 1717–1742.
- 14 H. Yue, C. Zhu, L. Huang, A. Dewanji and M. Rueping, *Chem. Commun.*, 2022, **58**, 171–184.
- 15 D. P. Lubov, E. P. Talsi and K. P. Bryliakov, *Russ. Chem. Rev.*, 2020, **89**, 587.
- 16 X. Jiang, S. Wang, G. Guo and B. Lu, *Chin. J. Org. Chem.*, 2017, **37**, 841.
- 17 T. Zhang, Y.-H. Wu, N.-X. Wang and Y. Xing, *Synthesis*, 2019, **51**, 4531–4548.
- 18 H. Targhan, P. Evans and K. Bahrami, *J. Ind. Eng. Chem.*, 2021, **104**, 295–332.
- 19 H. Mimoun, *Angew. Chem., Int. Ed.*, 1982, **21**, 734–750.
- 20 X. Zhang, M. Wang, P. Li and L. Wang, *Chem. Commun.*, 2014, **50**, 8006–8009.
- 21 L. Wang, K. Zhu, Q. Chen and M. He, *J. Org. Chem.*, 2014, **79**, 11780–11786.
- 22 S. Guo, J.-T. Yu, Q. Dai, H. Yang and J. Cheng, *Chem. Commun.*, 2014, **50**, 6240–6242.
- 23 W. C. Yang, P. Dai, K. Luo and L. Wu, *Adv. Synth. Catal.*, 2016, **358**, 3184–3190.
- 24 F. Mou, Y. Sun, W. Jin, Y. Zhang, B. Wang, Z. Liu, L. Guo, J. Huang and C. Liu, *RSC Adv.*, 2017, **7**, 23041–23045.
- 25 B. Xiong, G. Wang, C. Zhou, Y. Liu, P. Zhang and K. Tang, *J. Org. Chem.*, 2018, **83**, 993–999.
- 26 H. Jiang, X. Tang, S. Liu, L. Wang, H. Shen, J. Yang, H. Wang and Q.-W. Gui, *Org. Biomol. Chem.*, 2019, **17**, 10223–10227.
- 27 W.-K. Luo, C.-L. Xu and L. Yang, *Tetrahedron Lett.*, 2019, **60**, 151328.
- 28 A. Dandia, D. K. Mahawar, R. Sharma, R. S. Badgoti, K. S. Rathore and V. Parewa, *Appl. Organomet. Chem.*, 2019, **33**, e5232.
- 29 Y. Zhang, G. Hu, D. Ma, P. Xu, Y. Gao and Y. Zhao, *Chem. Commun.*, 2016, **52**, 2815–2818.
- 30 Y. Dong, J. Yang, S. He, Z.-C. Shi, Y. Wang, X.-M. Zhang and J.-Y. Wang, *RSC Adv.*, 2019, **9**, 27588–27592.
- 31 J. Z. Li, L. Mei, X. E. Cai, C. C. Zhang, T. T. Cao, X. J. Huang, Y. L. Liu and W. T. Wei, *Adv. Synth. Catal.*, 2022, **364**, 2080–2085.
- 32 M.-X. Sun, Y.-F. Wang, B.-H. Xu, X.-Q. Ma and S.-J. Zhang, *Org. Biomol. Chem.*, 2018, **16**, 1971–1975.
- 33 J.-j. Ma, W.-b. Yi, G.-p. Lu and C. Cai, *Org. Biomol. Chem.*, 2015, **13**, 2890–2894.
- 34 P. Kumar, T. Guntreddi, R. Singh and K. N. Singh, *Org. Chem. Front.*, 2017, **4**, 147–150.
- 35 T. Liu, K. B. Gan, R.-L. Zhong, X. He and F. Y. Kwong, *Org. Lett.*, 2022, **24**, 6805–6809.
- 36 X. Zhang, W. Li, Y. Yu, M. Luo, H. Bai, L. Shi and H. Li, *Green Chem.*, 2024, **26**, 2207–2212.
- 37 X. Liu, D. Wang, J. Garo, J.-M. Sotiropoulos and M. Taillefer, *Org. Chem. Front.*, 2024, **11**, 775–780.
- 38 B. Neil, L. Saadi, L. Fensterbank and C. Chauvier, *Angew. Chem.*, 2023, **135**, e202306115.
- 39 C. Weindl and L. Hintermann, *Chem.–Eur. J.*, 2024, e202401034.



40 N. Rezaei, E. Sheikhi and P. R. Ranjbar, *Synlett*, 2018, **29**, 912–917.

41 L. Bering, K. Jeyakumar and A. P. Antonchick, *Org. Lett.*, 2018, **20**, 3911–3914.

42 H. Shimojo, K. Moriyama and H. Togo, *Synthesis*, 2015, **47**, 1280–1290.

43 D. Wu, Y. Duan, K. Liang, H. Yin and F.-X. Chen, *Chem. Commun.*, 2021, **57**, 9938–9941.

44 Y. Yang, Y. Yu, Y. Wang, Q. Zhang and D. Li, *Tetrahedron*, 2018, **74**, 1085–1091.

45 F. Wu, X. Han, X. Li, X. Shen, C. Wang, Z. Tian, B. Cheng, J. Zhang, L. Sheng and H. Zhai, *Commun. Chem.*, 2021, **4**, 46.

46 D. Pan, Z. Pan, Z. Hu, M. Li, X. Hu, L. Jin, N. Sun, B. Hu and Z. Shen, *Eur. J. Org. Chem.*, 2019, **2019**, 5650–5655.

47 Z. Liu, M. Li, G. Deng, W. Wei, P. Feng, Q. Zi, T. Li, H. Zhang, X. Yang and P. J. Walsh, *Chem. Sci.*, 2020, **11**, 7619–7625.

48 Q.-Y. Meng, T. E. Schirmer, A. L. Berger, K. Donabauer and B. König, *J. Am. Chem. Soc.*, 2019, **141**, 11393–11397.

49 Y. Guo, J. Qi, H. Guo, R. Liu and R. Zhou, *J. Org. Chem.*, 2024, **89**, 2032–2038.

50 J. Shen, N. Li, Y. Yu and C. Ma, *Org. Lett.*, 2019, **21**, 7179–7183.

51 H. Jiang, C. Zang, H. Cheng, B. Sun and X. Gao, *Catal. Sci. Technol.*, 2021, **11**, 7955–7962.

52 F. Wu, J. P. Ariyarathna, N. Kaur, N.-E. Alom, M. L. Kennell, O. H. Bassiouni and W. Li, *Org. Lett.*, 2020, **22**, 2135–2140.

53 J. Inoa, M. Patel, G. Dominici, R. Eldabagh, A. Patel, J. Lee and Y. Xing, *J. Org. Chem.*, 2020, **85**, 6181–6187.

54 Y. Zhang, S. Qin, N. Claes, W. Schilling, P. K. Sahoo, H. V. Ching, A. Jaworski, F. Llemière, A. Slabon, S. Van Doorslaer, S. Bals and S. Das, *ACS Sustainable Chem. Eng.*, 2021, **10**, 530–540.

55 A. R. Spencer, R. Grainger, A. Panigrahi, T. J. Lepper, K. Bentkowska and I. Larrosa, *Chem. Commun.*, 2020, **56**, 14479–14482.

56 J. Gui, M. Sun, H. Wu, J. Li, J. Yang and Z. Wang, *Org. Chem. Front.*, 2022, **9**, 4569–4574.

57 J. Grover, G. Prakash, C. Teja, G. K. Lahiri and D. Maiti, *Green Chem.*, 2023, **25**, 3431–3436.

58 Y. Qin, T. Zhang, H. V. Ching, G. S. Raman and S. Das, *Chem.*, 2022, **8**, 2472–2484.

59 A. Chhikara, N. Kaur, E. B. Wolke, E. A. Boes, A. M. Nguyen, J. P. Ariyarathna, P. Baskaran, C. E. Villa, A. H. Pham, V. J. Kremenets, S. R. Kutcher, J. T. Truong and W. Li, *Org. Lett.*, 2024, **26**, 84–88.

60 E. Le Saux, M. Zanini and P. Melchiorre, *J. Am. Chem. Soc.*, 2022, **144**, 1113–1118.

61 Y. Zhang, P. K. Sahoo, P. Ren, Y. Qin, R. Cauwenbergh, P. Nimmemeers, G. SivaRaman, S. Van Passel, A. Guidetti and S. Das, *Chem. Commun.*, 2022, **58**, 11454–11457.

62 P. K. Sahoo, Y. Zhang, Y. Qin, P. Ren, R. Cauwenbergh, G. S. Raman and S. Das, *J. Catal.*, 2023, **425**, 80–88.

63 C. Bo, F. Chen, Q. Bu, Z.-H. Du, M. Li, B. Dai and N. Liu, *J. Org. Chem.*, 2023, **88**, 3532–3538.

64 X. Zhao, X. Yu, M. Liu, Y. Huo, S. Ji, X. Li and Q. Chen, *J. Org. Chem.*, 2023, **88**, 2612–2620.

65 K. Almagambetova, K. Murugesan and M. Rueping, *ACS Catal.*, 2024, **14**, 12664–12670.

66 Y. Li, S. Guo, Q.-H. Li and K. Zheng, *Nat. Commun.*, 2023, **14**, 6225.

67 R. Hayashi, A. Shimizu, Y. Song, Y. Ashikari, T. Nokami and J. i. Yoshida, *Chem.-Eur. J.*, 2017, **23**, 61–64.

68 Z. W. Hou, D. J. Liu, P. Xiong, X. L. Lai, J. Song and H. C. Xu, *Angew. Chem., Int. Ed.*, 2021, **60**, 2943–2947.

69 P. Xiong, H.-B. Zhao, X.-T. Fan, L.-H. Jie, H. Long, P. Xu, Z.-J. Liu, Z.-J. Wu, J. Cheng and H.-C. Xu, *Nat. Commun.*, 2020, **11**, 2706.

70 Y. Meng, E. Gnanamani and R. N. Zare, *J. Am. Chem. Soc.*, 2022, **144**, 19709–19713.

71 S. Zhang, Y. Li, T. Wang, M. Li, L. Wen and W. Guo, *Org. Lett.*, 2022, **24**, 1742–1746.

72 S. Tang, R. Guillot, L. Grimaud, M. R. Vitale and G. Vincent, *Org. Lett.*, 2022, **24**, 2125–2130.

73 Y. Zhang, X. Sun, J.-H. Su, T. Li, C. Du, K. Li, Q. Sun, Z. Zha and Z. Wang, *Org. Lett.*, 2023, **25**, 5067–5072.

74 X.-W. Wang, Y. Deng, R.-X. Li, J.-F. Lv, M.-Q.-H. Fu, Z. Guan, Y.-N. Zhao and Y.-H. He, *ACS Sustainable Chem. Eng.*, 2023, **11**, 1624–1630.

75 H. Wang, K. Liang, W. Xiong, S. Samanta, W. Li and A. Lei, *Sci. Adv.*, 2020, **6**, eaaz0590.

76 Y. Liang, X. Zhan, F. Li, H. Bi, W. Fan, S. Zhang and M.-B. Li, *Chem Catal.*, 2023, **3**, 100582.

77 P. Qian, D. Zhu, X. Wang, Q. Sun and S. Zhang, *J. Org. Chem.*, 2024, **89**, 6395–6404.

